University of Tennessee, Knoxville

TRACE: Tennessee Research and Creative Exchange

Doctoral Dissertations

Graduate School

5-2006

Cellulosic Fibers and Nonwovens from Solutions: Processing and Properties

Atul Dahiya
University of ten

Follow this and additional works at: https://trace.tennessee.edu/utk_graddiss

Part of the Materials Science and Engineering Commons

Recommended Citation

Dahiya, Atul, "Cellulosic Fibers and Nonwovens from Solutions: Processing and Properties. " PhD diss., University of Tennessee, 2006.
https://trace.tennessee.edu/utk_graddiss/4258

This Dissertation is brought to you for free and open access by the Graduate School at TRACE: Tennessee Research and Creative Exchange. It has been accepted for inclusion in Doctoral Dissertations by an authorized administrator of TRACE: Tennessee Research and Creative Exchange. For more information, please contact trace@utk.edu.

To the Graduate Council:

I am submitting herewith a dissertation written by Atul Dahiya entitled "Cellulosic Fibers and Nonwovens from Solutions: Processing and Properties." I have examined the final electronic copy of this dissertation for form and content and recommend that it be accepted in partial fulfillment of the requirements for the degree of Doctor of Philosophy, with a major in Materials Science and Engineering.

Billie J. Collier, Major Professor

We have read this dissertation and recommend its acceptance:

Simioan Petrovan, Randall R. Bresee, John R. Collier

Accepted for the Council:

Carolyn R. Hodges

Vice Provost and Dean of the Graduate School

(Original signatures are on file with official student records.)

To the Graduate Council:

I am submitting herewith a dissertation written by Atul Dahiya entitled "Cellulosic Fibers and Nonwovens from Solutions: Processing and Properties." I have examined the final paper copy of this dissertation for form and content and recommend that it be accepted in partial fulfillment of the requirements for the degree of Doctor of Philosophy, with a major in Material Science and Engineering.

Billie J. Collier, Major Professor

We have read this dissertation
and recommend its acceptance:

Accepted for the Council:

Vice Chancellor and Dean of
Graduate Studies

Thesis
2006b
.D24

CELLULOSIC FIBERS AND NONWOVENS FROM SOLUTIONS: PROCESSING AND PROPERTIES

A Dissertation
Presented for the
Doctor of Philosophy
Degree
The University of Tennessee, Knoxville

Atul Dahiya
May 2006

ACKNOWLEDGEMENTS

The author expresses his profound sense of gratitude to Dr. Billie J. Collier, the chairperson of his advisory committee, for her help and invaluable guidance throughout this study. Her unstinted cooperation and encouragement were of utmost importance for the completion of this study. He would also like to thank Dr. John R. Collier and Dr. Simioan Petrovan for their valuable time, guidance and constant encouragement in the successful completion of the work. He would also like to highly appreciate Dr. Randall R. Bresee for his assistance and willingness to serve on the graduate advisory committee.

He extends his thanks to Mr. Chris Eash, Research Associate, Textile and Nonwovens and Development Centre, for the help he offered in setting up the melt blowing line used for this study. Nonetheless, the author is grateful to Ms. Rhea Sammons and Ms. Joy Watson, graduate students in Chemical Engineering, University of Tennessee, for the help they rendered during the various stages of this study. Last but not least he would like to extend a sincere thanks to all those who came along in this endeavor and made this study a success.

ABSTRACT

Cellulose is a renewable and bio-based material source extracted from wood that has the potential to generate value added products such as composites, fibers, and nonwoven textiles. This research was focused on the potential of cellulose as the raw material for fiber spinning and melt blowing of nonwovens. The cellulose was dissolved in two different benign solvents: the amine oxide 4-N-methyl morpholine oxide monohydrate (NMMO•H_2O) (lyocell process); and the ionic liquid (IL) 1-butyl-3-methylimidazolium chloride ([C_4MIM]Cl). The solvents have essentially no vapor pressure and are biologically degradable, making them environmentally advantageous for manufacturing processes. The objectives of this research were to:

- characterize solutions of NMMO and [C_4MIM]Cl
- develop processing techniques to melt blow nonwoven webs from cellulose using NMMO as a solvent
- electrospin cellulosic fibers from the [C_4MIM]Cl solvent
- spin cellulosic single fibers from the [C_4MIM]Cl solvent

Different concentration solutions of cellulose in NMMO and [C_4MIM]Cl were initially characterized rheologically and thermally to understand their behavior under different conditions of stress, strain, and temperature. Results were used to determine processing conditions and concentrations for the melt blowing, fiber spinning, and electrospinning experiments.

The cellulosic nonwoven webs and fibers were characterized for their physical and optical properties such as tensile strength, water absorbency, fiber diameter, and fiber surface. Thermal properties were also measured by thermogravimetric analysis, differential scanning calorimetry, and dynamic mechanical analysis.

Lyocell webs were successfully melt blown from the 14% cellulose solution. Basis weights of the webs were 27, 79, and 141 g/m^2 and thicknesses ranged from 0.3-0.9 mm, depending on die temperatures and die to collector distance. The average fiber diameter achieved was 2.3 microns. The 6% lyocell solutions exhibited poor spinability and did not form nonwoven webs. The electrospun nonwoven webs obtained were evaluated for fiber diameter and surface/web structure using scanning electron microscopy (SEM). The fibers obtained were in the range of 17-25 microns and the fiber surfaces and shapes varied with spinning conditions. A capillary rheometer was used to spin single fibers from [C_4MIM]Cl. Circular fibers in diameter ranging from 12-84 microns were obtained.

Potential applications of these melt blown and electrospun webs include hygiene and medical products where softness, moisture absorbance, and barrier properties are desirable. Apparel is a new and growing market for nonwovens and the aesthetics and drapeability of regenerated cellulosic fibers should have appeal.

TABLE OF CONTENTS

Chapter	Page
CHAPTER 1 INTRODUCTION	**1**
1.1 BACKGROUND	1
1.2 MOTIVATION FOR THE PRESENTED WORK	2
CHAPTER 2 LITERATURE REVIEW	**4**
2.1 CELLULOSE	4
2.1.1 WOOD STRUCTURE	5
2.1.2 WOOD CHEMISTRY	6
2.2 LYOCELL/NMMO (4-N-METHYL MORPHOLINE OXIDE)	10
2.2.1 NMMO	13
2.2.2 DISSOLUTION MECHANISM	15
2.2.3 LYOCELL PROCESSING	16
2.2.4 RHEOLOGY	20
2.2.4.1 SHEAR FLOW	21
2.2.4.2 ELONGATIONAL FLOW	23
2.2.4.3 ORIENTATION	26
2.2.5 FIBER PROPERTIES	27
2.2.6 APPLICATION	29
2.3 IONIC LIQUIDS	30
2.3.1 PROPERTIES	32
2.3.2 DISSOLUTION MECHANISM	33
2.3.3 SYNTHESIS	34
2.3.4 IL/CELLULOSE PROCESSING	36

2.4 ELECTROSPINNING 36

2.4.1 INTRODUCTION 36
2.4.2 PRINCIPLE 39
2.4.3 ORIENTATION 41
2.4.3.1 PROCESS VARIABLES 42
2.4.4 CELLULOSE ELECTROSPINNING 43

2.5 MELT BLOWING 43

2.5.1 INTODUCTION TO MELT BLOWING PROCESS 43
2.5.2 ELEMENTS OF MELT BLOWING PROCESS 46
2.5.2.1 EXTRUDER 46
2.5.2.1.1 TWIN SCREW EXTRUDER 47
2.5.2.1.2 VENTED EXTRUSION 49
2.5.2.2 GEAR PUMP 49
2.5.2.3 DIE ASSEMBLY 49
2.5.2.4 WEB FORMING 50
2.5.2.5 WINDING 52
2.5.3 PROCESS VARIABLES 52
2.5.3.1 MACHINE VARIABLES 52
2.5.3.2 OFF-LINE VARIABLES 53
2.5.3.3 MATERIAL VARIABLES 53
2.5.4 ORIENTATION 54

CHAPTER 3 PROCEDURES 57

3.1 SAMPLE PREPARATION 57

3.1.1 PREPARATION OF LYOCELL SOLUTIONS 57
3.1.2 PREPARATION OF IL/CELLULOSE SOLUTION 58

3.2 LYOCELL MELTBLOWING 59

3.3 ELECTROSPINNING OF IL/CELLULOSE 61

3.4 ACER ASSISTED SPINNING OF IL/CELLULOSE 61

3.5 CHARACTERIZATION TECHNIQUES 64

3.5.1 THERMAL ANALYSIS 64
3.5.1.1 DIFFERENTIAL SCANNING CALORIMETR (DSC) 64
3.5.1.2 THERMOGRAVIMETRIC ANALYSIS (TGA) 64
3.5.2 BASIS WEIGHT 66
3.5.3 TENSILE STRENGTH 66
3.5.4 THICKNESS 66
3.5.5 ABSORBENCY 66
3.5.6 PORE SIZE 68
3.5.7 CONTACT ANGLE 69
3.5.8 SCANNING ELECTRON MICROSCPE (SEM) 69
3.5.9 X-RAY DIFFRACTION 71

CHAPTER 4 RESULTS AND DISCUSSIONS 72

4.1 IL/CELLULOSE RHEOLOGY 72

4.2 THERMAL ANALYSIS 72

4.2.1 DSC 72
4.2.2 TGA 80

4.3 LYOCELL MELT BLOWING 86

4.3.1 LYOCELL MB NONWOVEN WEB CHARACTERIZATION 87
4.3.1.1 TENSILE STRENGTH 89
4.3.1.2 ATS ABSORBENCY 89
4.3.1.3 PMI CAPILLARY FLOW POROMETER 94

4.3.1.4 CONTACT ANGLE 97

4.4 IL/CELLULOSE ELECTROSPINNING 97

4.4.1 IL/CELLULOSE ELECTROSPUN WEB CHARACTERIZATION 99

4.5 IL/CELLULOSE ACER ASSITED SPINNING 101

4.6 CRYSTALLINITY 104

CHAPTER 5 CONCLUSIONS AND FUTURE WORK 108

5.1 CONCLUSIONS 108

5.2 FUTURE WORK 109

REFERENCES 110

VITA 128

LIST OF TABLES

Table	Page
TABLE 2.1 COMPOSITION OF WOOD	7
TABLE 2.2 FIBER PROPERTIES	28
TABLE 3.1 DIFFERENT PROCESSING CONDITIONS	60
TABLE 4.1 TEST RESULTS FOR LYOCELL WEBS	90
TABLE 4.2 PMI MEASUREMENTS	95
TABLE 4.3 CONTACT ANGLE MEASUREMENTS	98
TABLE 4.4 PROCESSING CONDITIONS FOR IL ELECTROSPINNING	98
TABLE 4.5 PROCESSING CONDITION FOR ACER ASSISTED SPINNING	102
TABLE 4.6 FIBER BUNDLE STRENGTH	102

LIST OF FIGURES

Figure	Page
FIGURE 2.1 SCHEMATIC OF PLANT CELL WALL	7
FIGURE 2.2 MOLECULAR STRUCTURE OF CELLULOSE	7
FIGURE 2.3 CELLULOSE FIBER MAKING PROCESSES	12
FIGURE 2.4 4-N-METHYL MORPHOLINE OXIDE (NMMO)	14
FIGURE 2.5 FORMATION OF N-METHYL MORPHOLINE OXIDE	14
FIGURE 2.6 PROPYL GALLATE	17
FIGURE 2.7. COMPARATIVE COMPLEX VISCOSITIES	17
FIGURE 2.8. COMPARATIVE ELONGATIONAL VISCOSITIES	18
FIGURE 2.9. PARALLEL PLATE GEOMETRY	22
FIGURE 2.10. 1-ALKYL-3-IMIDAZOLIUM HALIDE SYNTHESIS	35
FIGURE 2.11 RELATIONSHIP BETWEEN FIBER DIAMETER AND SURFACE AREA OF NYLON 6,6 FIBER	38
FIGURE 2.12 SCHEMATIC OF LABORATORY SCALE ELECTROSPINNING SETUP	40
FIGURE 2.13 SCHEMATIC FOR MB PROCESS	45
FIGURE 2.14 SCHEMATIC SHOWING THE AIR FLOW THROUGH THE DIE ASSEMBLY	51
FIGURE 2.15 BIREFRINGENCE OF FIBERS IN RELATION TO DISTANCE FROM THE DIE	56
FIGURE 3.1 TWIN SCREW MB SYSTEM	60
FIGURE 3.2.ELECTROSPINNING SETUP	62
FIGURE 3.3 SCHEMATIC OF A ACER ASSISTED SPINNING SETUP	63
FIGURE 3.4 SCHEMATIC OF ORIENTATION OCCURRING IN HYPERBOLIC DIE	65
FIGURE 3.5 WILHELMY METHOD	70
FIGURE 4.1 IL/CELLULOSE VISCOSITY CURVES AT 80°C	73

FIGURE 4.2 IL/CELLULOSE VISCOSITY CURVES AT 90°C 74
FIGURE 4.3 IL/CELLULOSE VISCOSITY CURVES AT 100°C 75
FIGURE 4.4 DSC GRAPHS FOR LYOCELL (NMMO/CELLULOSE) 77
FIGURE 4.5 DSC GRAPHS FOR IL/CELLULOSE 78
FIGURE 4.6 DSC GRAPHS FOR IL/CELLULOSE FROZEN IN LIQUID NITROGEN 79
FIGURE 4.7 TGA FOR LYOCELL MB WEBS WASHED IN MAY 2004 81
FIGURE 4.8 TGA FOR LYOCELL MB WEBS WASHED IN FEBRUARY 2005 82
FIGURE 4.9 TGA FOR LYOCELL MB WEBS 83
FIGURE 4.10 TGA FOR IL/CELLULOSE SOLUTION 84
FIGURE 4.11 TGA FOR NMMO•H_2O AND IL 85
FIGURE 4.12 OUTLINE DIAGRAM NMMO/H_2O (50/50) RUN 88
FIGURE 4.13 ATS ABSORBENCY MEASUREMENTS FOR 400 SECONDS 90
FIGURE 4.14 SEM MICROGRAPHS OF 14% LYOCELL MB NONWOVEN WEBS WASHED IN MAY 2004 91
FIGURE 4.15 SEM MICROGRAPHS OF 14% LYOCELL MB NONWOVEN WEBS WASHED IN FEBRUARY 2005 92
FIGURE 4.16 ATS ABSORBENCY MEASUREMENTS FOR FIRST 20 SECONDS 93
FIGURE 4.17 SEM MICROGRAPHS UNWASHED 14% LYOCELL MB NONWOVEN WEBS 96
FIGURE 4.18 SEM MICROGRAPHS OF IL/CELLULOSE ELECTROSPUN NONWOVEN WEBS 100
FIGURE 4.19 SEM MICROGRAPHS OF IL/CELLULOSE FIBERS 103
FIGURE 4.20 CROSS SECTION OF THE FIBERS OBTAINED BY MICROTOMING THE SAMPLES AND USING LEICA CONFOCAL LASER MICROSCOPE 105
FIGURE 4.21 X-RAY MICROGRAPHS 106

FIGURE 4.22 INTENSITY VS SCATTERING 107

Chapter 1 Introduction

1.1 BACKGROUND

Cellulose is the most abundant naturally occurring biopolymer. The primary constituent in wood, it has also found applications in fibers, films, and composites. Regenerated cellulosic fibers such as rayon and acetate were commercial successes for most of the 20th century. Rayon fibers are 100% cellulose, whereas cellulose acetate contains acetate groups on the cellulose polymer.

The viscose and cuprammonium processes have been used for over a hundred years to make rayon fibers from cellulose. Neither is employed any longer in the U.S. because of the harsh chemicals used and pollutants generated in the waste stream. Manufacturing of rayon fibers with these processes does however continue in other countries. The viscose rayon process uses sodium hydroxide, sulfuric acid, and carbon disulfide (CS_2), emitting CS_2 and H_2S as the side products during the cellulose regeneration process. These emissions into the air and the waste stream are toxic and environmentally hazardous and have been an environmental concern for some time [1 - 3]. The cuprammonium rayon process uses a copper ammonium solvent, resulting in significant amounts of copper in the plant effluent. Producers have been unable to continue manufacturing these fibers in the U.S. because of the added costs of treatment or control of the emissions under tighter environmental regulations. At the same time, the desirable properties of rayon fibers have lead to

the exploration of alternative, more environmentally benign, processes for making these regenerated cellulosic fibers.

Several organic solvents have been investigated to determine their ability to dissolve cellulose. The cyclic amine oxide 4-N-methyl morpholine oxide (NMMO) and the ionic liquid (IL) 1-butyl-3-methylimidazolium chloride ([C_4MIM]Cl) are such solvents which directly dissolve cellulose and have been used commercially or experimentally to demonstrate spinnability. These solvents have essentially no vapor pressure and are biologically degradable, making them environmentally advantageous for manufacturing processes. They are thus safer to use and have the added economic advantage of being recoverable and reusable.

Lyocell is the generic name for fibers made by dissolving cellulose in NMMO. Lenzing Fibers presently manufactures lyocell fibers under the trade names Tencel® and Lenzing Lyocell®. These fibers have high absorbency, mechanical properties that make them appropriate for blending with other fibers, and they are suitable for different processing technologies such as knitting and weaving. Lyocell microfibers of 0.9 dtex have been successfully produced to give fabrics with high tenacity and a silk-like hand [4].

1.2 MOTIVATION FOR THE PRESENTED WORK

Melt blown (MB) nonwoven webs are known for their special properties such as softness and high fiber surface area, which provide good filtration and barrier properties. These characteristics are due largely to the fineness of the fibers formed

during the MB process. Currently MB fabrics are made primarily from synthetic polymers which are nonabsorbent and non-biodegradable. Cellulose is absorbent and, being a renewable source, is environmentally attractive. MB cellulosic webs should present a new type of nonwoven with desirable characteristics that enhance the softness and filtration properties. Weyerhaeuser Company has conducted pioneering research in melt blowing lyocell fibers [5 - 8]. So far the processes that have been developed for cellulosic nonwovens have been limited to making commercial fabric from fibers either by needlepunching or chemical bonding [4] and making nonwoven webs experimentally [7, 8].

Another method for achieving very fine fibers is electrospinning. Electrospinning is a technique where spinning of fibers is done under an electrostatic force field applied by a high voltage DC source. It is known to produce nanofibers having a diameter less than one micron.

The primary objective of this project was to develop a novel process for making a continuous nonwoven web using cellulose with a minimum number of steps involved so as to make it commercially viable. Melt blowing and electrospinning were investigated as techniques for producing webs of cellulosic microfibers. Two solvent systems were studied: NMMO and $[C_4MIM]Cl$.

Chapter 2 Literature Review

2.1 CELLULOSE

Wood is the main source of raw material for cellulose which is available in abundance, as nearly one third of the earth's total land area is covered by forests. Cellulose comprises roughly $1.5x10^{12}$ tons of the total annual biomass production [8-11]. The main polysaccharide in the cell wall of plants, cellulose is available in plenty and is nearly inexhaustible; it is the primary renewable resource. The use of cellulose in a number of products however is limited by its poor processability, low solubility, and inability to melt because of its molecular structure [12 - 14].

Pulp is the fibrous substance isolated from wood after the chemical pulping process. The pulping process involves controlled removal of the lignin, which is the substance holding the short fibers together in the wood structure. Most commonly, sulfites are used for this step, followed by an extraction of the hemicellulose by "cooking" the wood under pressure with various chemicals like sodium hydroxide and sodium sulfide at temperatures around 170-180°C for approximately 2-4 hours. In the cooking process the alkali causes the breakdown of lignin molecules which are soluble in the cooking liquor. Cooking is later followed by bleaching and purification at atmospheric pressure. Although there is never complete separation of the hemicellulose, some degradation occurs during the pulping process and the process usually results in 99% pure cellulose.

Both softwoods (coniferous wood) and hardwoods (deciduous wood) are used for pulping. Softwoods, however, predominate for several reasons. Hardwood is known to give non-uniform pulping due to its availability as mixed species that have different properties [15]. Also the chemical composition of hardwood makes it difficult for the pulping liquors to penetrate the structure during the pulping process. Another reason for not using hardwood is the difficulty in transporting it. River transportation is the most economical means of delivering wood to pulping plants, but is not ideal for hardwood because hardwoods have higher water absorbency compared to some of the softwoods.

2.1.1 WOOD STRUCTURE

Cellulose is found in the stalks, stems, trunks and all the woody portions of plant tissue. For pulping, it is the trunk part of the tree that is mainly used for obtaining cellulose and not the bark because the latter has very low cellulose content and high amounts of lignin and other compounds extractable with organic solvents and water. The trunk is composed of three components: xylem or wood, the cambium, and the bark. The structure of the wood varies with the age of the tree. The trunks of older trees have a denser structure in the inner part (heartwood) than in the outer sapwood.

Wood is composed of four structural components, viz. parenchyma cells, fibers, tracheids, and vessel elements. Parenchyma cells serve as storage and transportation cells for food and water, fibers are the structural supporting elements

responsible for giving the rigidity to the wood system, and the tracheids and vessels act as water transporters and also as mechanical structural elements for the wood. The cell wall structure for cotton and wood fibers is shown in Figure 2.1.

2.1.2 WOOD CHEMISTRY

Wood is composed of three basic elements: carbon (C) 50%, hydrogen (H) 4% and oxygen (O) 44%. There are also small amounts of nitrogen (<0.1%) and ash (approximately 0.3%) present in the wood [15]. The largest variation in wood composition is between species; within species, however, variation is very low. The three main components are cellulose, hemicelluloses, and lignin. The average amount of these components in wood that has had other minor substances extracted is given in Table 2.1 [15]. The extractives present in wood are pectins, methyl esters and waxes [16, 17].

Cellulose: The presence of cellulose in the fibrous material of wood was first noted by Payen in 1938 during its acid ammonia treatment [16, 18]. Since then abundant research has been conducted, but still there is not complete information available on its structural features and properties. Cellulose is the main constituent and structural component of plants and is also present in algae, fungi, bacteria and animals. Cellulose is a linear polysaccharide of high chain length, consisting of D-anhydroglucose units linked with 1,4-β-glucosidic bonds (Figure 2.2). The successive glucose rings are rotated through a 180° angle about the molecular axis, giving the anhydroglucose units a chair conformation. Cellulose is insoluble in water

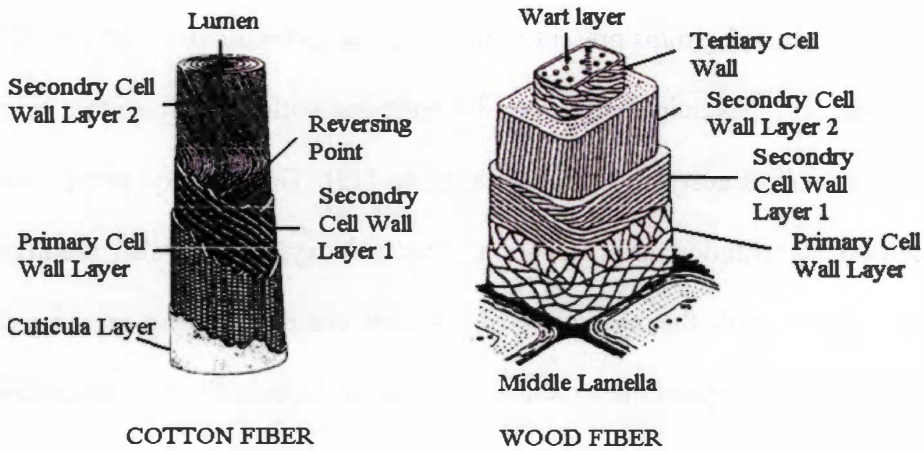

Figure 2.1 Schematic of plant cell wall [8, 19]

Table 2.1 Composition of wood

	Softwood	Hardwood
Cellulose	43	43
Hemicelluloses	28	35
Lignin	29	22

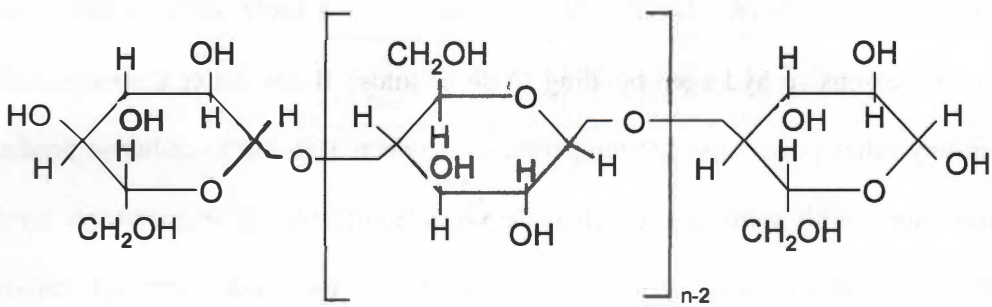

Figure 2.2 Molecular structure of cellulose

dilute alkali, and acids at room temperature.

The hydroxyl groups present in the cellulose molecule have the capability to undergo reaction as studied in the past by reactions with metallic sodium in liquid ammonia as well as acetylation and methylation [15]. The hydroxyl group can react by addition, substitution and oxidation. The hydroxyl groups also readily form hydrogen bonds with the hydroxyls of adjacent chains resulting in a crystalline structure. It is their crystalline structure that gives cellulosic fibers, both natural and manufactured, strength.

Cellulose exists in six different polymorphs out of which two polymorphs, cellulose I and cellulose II, are of importance. The polymer chains in cellulose I are parallel in the unit cell, whereas cellulose II has an antiparallel conformation [20]. Cellulose I is the naturally occurring form, which can be transformed to cellulose II by either of two methods: treatment with strong sodium hydroxide (mercerization), resulting in swollen fibers; or dissolving it in a solvent and precipitating it in water or some other solvent [9, 16, 19 - 22]. Cellulose II is a more stable structure as it provides extensive hydrogen bonding. Also cellulose II has better thermal stability then any other polymorph. At temperatures between 100-200°C cellulose produces gases along with some tar and then degrades completely at temperatures around 300°C or more by giving off carbon dioxide, carbon monoxide, carbonyl, carboxyl and hydroperoxide groups along with low molecular weight compounds and intermediate decomposition products [23, 24].

Hemicelluloses: It is the noncellulosic polysaccharide part of wood, and occurs in close association with cellulose having a structure very close to that of cellulose. This makes it difficult to define a boundary between glucosidic and non-glucosidic components. Hemicelluloses are highly branched polymers compared to cellulose which is very linear [16]. The branching of hemicelluloses is due to the presence of different polysaccharides, among which are: D-glucose, D-xylose, D-mannose, L-arabinose, D-galactose, D-glucuronic acid, and D-galacturonic acid [6]. Hemicelluloses are located throughout the cell wall, in the middle of the lamella, and in the outer part of the cell wall. They are amorphous in structure, but when treated chemically it tend to crystallize, making it difficult to separate them from cellulose during the pulping process [15]. They can be extracted from the wood system by alkaline treatment.

Lignin: It constitutes 20-35% of the wood, depending on the species and rate of growth. Lignin exists as an amorphous structure in the wood. Carbon (63-67%), oxygen (27-32%) and hydrogen (5-6%) are three basic elements present in lignin. It has a complex structure consisting of aliphatic and aromatic constituents and surrounds the fiber as a sheath [16, 25]. The methoxyl group is the main characteristic group of lignin, and excepting a small amount found in hemicellulose, lignin is responsible for over 90% of methoxyl content of the wood [15]. Of the three components in wood systems, lignin is the least desirable because it has no immediate use. Since it constitutes a major part of wood, however, there is growing

interest in studying the chemistry of lignin and investigating potentially useful applications.

Cellulose molecules form a linear framework and are partly crystalline aggregates possessing a certain degree of stiffness even when in a molecular solution, whereas hemicellulose and lignin are amorphous structures encrusting the cell wall. Compared to lignin, hemicellulose is deposited at an earlier stage, and as it is more related to cellulose in structure, it is found to be more internally fused with the cellulose.

Cellulose is available in different degrees of polymerization (DP). In cellulose DP is the number of anhydroglucose units per molecule. Dilute solution viscometry is used to measure the DP of the pulps using TAPPI standard T206 which makes use of a cuprammonium hydroxide solution [23]. The higher the DP of a cellulosic fiber, higher is the tenacity [23]. Lower DP cellulose sources dissolve more easily in NMMO compared to an upper DP limit for achieving appropriate solution viscosities for spinning. Naturally occurring cellulose has an approximate DP of 10,000 anhydroglucose units in wood and 15,000 in cotton cellulose [20, 26].

2.2 LYOCELL/NMMO (4-N-METHYL MORPHOLINE OXIDE)

Lyocell is the generic fiber name given to a new class of rayon fibers produced by dissolving cellulose in 4-N-methyl morpholine oxide monohydrate ($NMMO \bullet H_2O$). It is appropriate to name these fibers lyocell due to lyotropic (rigid crystalline) nature of the cellulose solutions [27]. The term lyocell however is now

generally applied to the process, the cellulose fibers it produces, and the solution of NMMO and cellulose. Presently there are several full scale operating plants in Europe and Asia involved in the manufacturing of cellulose fibers using the lyocell process [28 - 31]. In the 1980s NMMO was discovered as one of the potential solvents for dissolving cellulose. It was not until 1991 however that lyocell fibers were first commercially developed by Courtaulds Fibers in Britain and produced under the trade name Tencel®. Lenzing Lyocell® is another commercially available lyocell fiber manufactured by Lenzing Fibers [4].

Until recently, regenerated cellulosic fibers were produced by the viscose wet spinning process. It involves derivatization of cellulose with carbon disulfide, dissolution in sodium hydroxide and spinning into a sulfuric acid bath. This process has low productivity, is energy intensive, as it involves several purification and waste treatment steps and is environmentally unsafe as it uses harmful chemicals that are discharged into the waste stream [32]. A comparison of the process differences between viscose and lyocell is shown in Figure 2.3. Other manufactured cellulosic fibers are:

- Cuprammonium rayon: cellulose is dissolved in cuprammonium hydroxide and spun into a water bath.

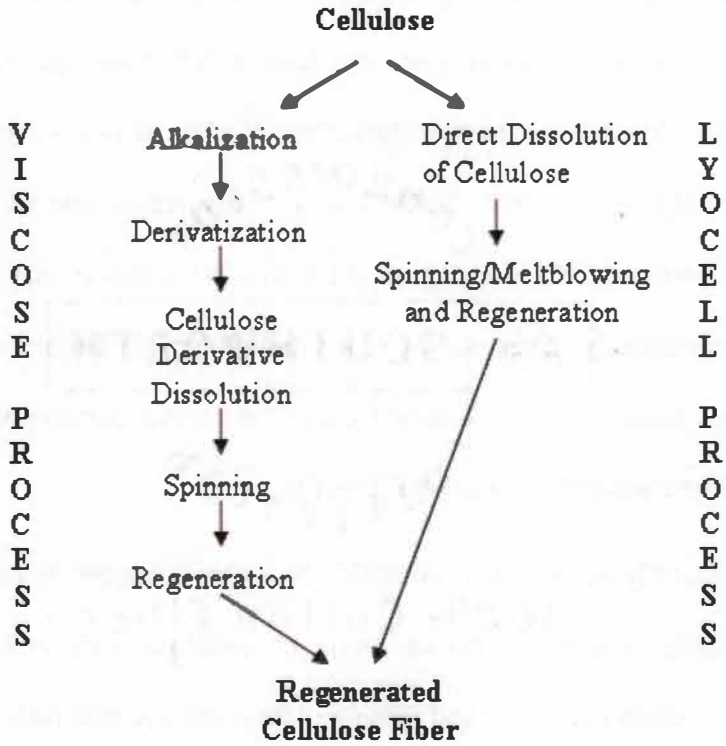

Figure 2.3 Cellulose fiber making processes

- Acetate (secondary cellulose acetate): cellulose is reacted with acetic anhydride to acetylate 74-92% of the hydroxyl groups. The acetate polymer is dissolved in acetone and dry spun.
- Triacetate (cellulose triacetate): produced by the same process as the acetate but atleast 92% of the hydroxyl groups are acetylated.

2.2.1 NMMO

NMMO is a cyclic aliphatic tertiary amine oxide as shown in Figure 2.4 and is highly polar in nature. The polarity is due to the highly polar N-O group, which makes the molecule soluble in water and has the ability to form hydrogen bonds. NMMO in its aqueous from has the capability of dissolving cellulose physically without undergoing any chemical reaction, derivatization or complexation [33, 34]. NMMO is highly oxidative and has an explosive tendency at temperatures above 180°C. The melting point of pure NMMO is 170°C, while that of the monohydrate form (water content 13.3 wt %) is 74°C.

NMMO is commercially produced by the methylation and oxidation of N-methylmorpholine with aqueous hydrogen peroxide (Figure 2.5). N-methyl morpholine is obtained by reaction between diethylene glycol and ammonia. NMMO is available in 50(water):50(NMMO) ratios. This solvent is benign, has essentially no vapor pressure and is biologically degradable, making it environmentally advantageous for manufacturing processes. The biodegradable nature of NMMO has

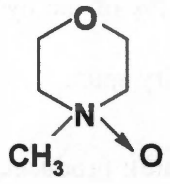

Figure 2.4 4-N-methyl morpholine oxide (NMMO)

$$O(C_4H_6)\,NCH_3 \xrightarrow[CO_2]{H_2O_2} O(C_4H_6)(NO)CH_3 + H_2O$$

N-Methyl morpholine N-Methyl morpholine oxide

Figure 2.5 Formation of N-methyl morpholine oxide [19]

been studied in the past by successfully biologically degrading the NMMO via microorganisms in conventional waste water treatment plants [35].

2.2.2 DISSOLUTION MECHANISM

In order to dissolve a solid material in a solvent system, the intermolecular attraction between the species, i.e. the solid and the solvent system, should be greater than the attractive forces within each single species. In this case the cellulose undergoes dissolution without any chemical reaction. A small amount of propyl gallate (PG) (1% wt of cellulose) is added to the cellulose before dissolution as a stabilizer.

The dissolution of cellulose in NMM•H_2O takes place by the disruption of the intermolecular and intramolecular hydrogen bonds in the cellulose molecule, which then later is followed by new hydrogen bond formations between NMMO and cellulose [28 - 30, 36]. The solvation process of cellulose in NMMO•H_2O is believed to occur in two stages: first is dissolution is of the readily accessible cellulose areas with simultaneous swelling; and second is the dissolving of the crystalline regions [37].

Ideally, the dissolution of cellulose in NMMO•H_2O should be a physical process with no side reactions or chemical changes. However in reality at high temperatures it results in cellulose degradation and discoloration with some byproducts, along with accelerated decomposition of NMMO [38]. This degradation

and yellowing of lyocell at high temperature is due to the presence of chromophores from side reactions because of the oxidative nature of NMMO [29, 39]. PG is the primary stabilizer used commercially (Figure 2.6). A phenolic antioxidant, it reacts with radicals forming relatively stable phenoxyl radicals [38].

2.2.3 LYOCELL PROCESSING

Lyocell solutions have been shown to exhibit rheological properties similar to those of polymer melts as shown in Figure 2.7 - Figure 2.8 [40 - 44]. They are therefore amenable to existing extrusion processes with little modification [45 - 48]. Centrifugal spinning, dry jet wet spinning and melt blowing are the techniques that have been used by researchers to produce lyocell fibers. The different steps involved in the manufacturing of regenerated cellulosic films/fibers/nonwovens webs by the lyocell process are:

- Preparation of the homogenous NMMO•H_2O/cellulose solution
- Extrusion of the lyocell solution (at 100-140°C) through a single or multiple hole die with additional attachment/capabilities for meltblowing a nonwoven web
- Passing cellulose fibers through a precipitation bath for coagulation of the fibers

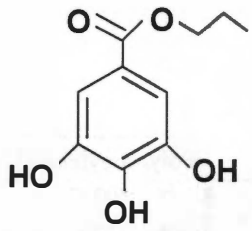

Figure 2.6 Propyl gallate

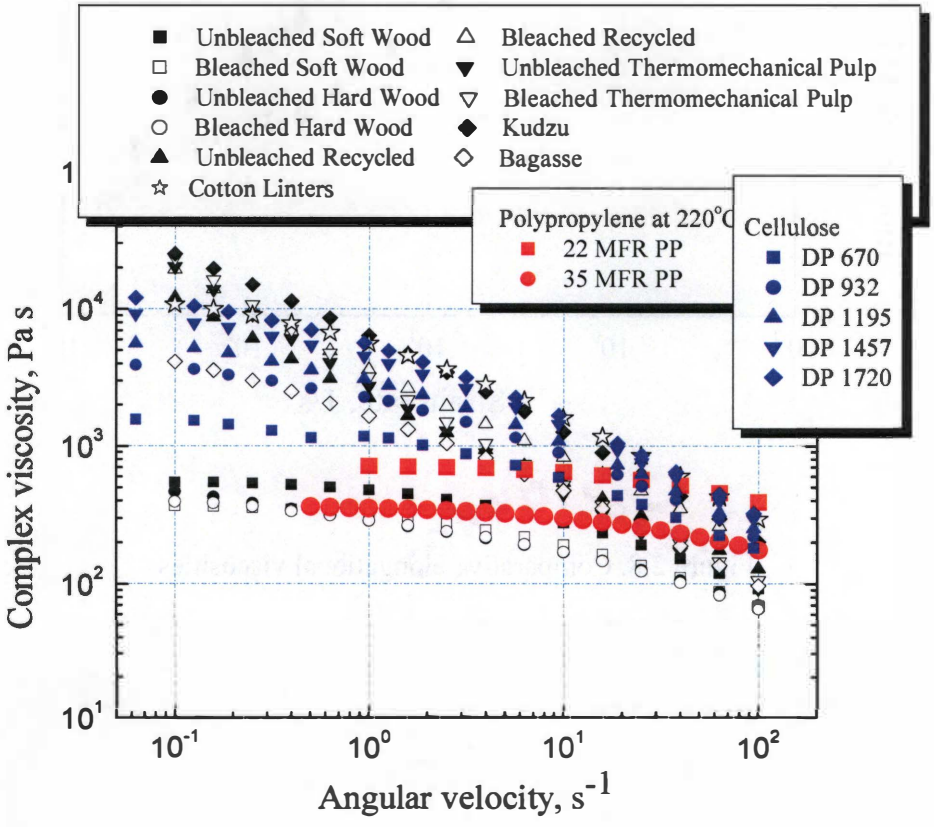

Figure 2.7. Comparative complex viscosities

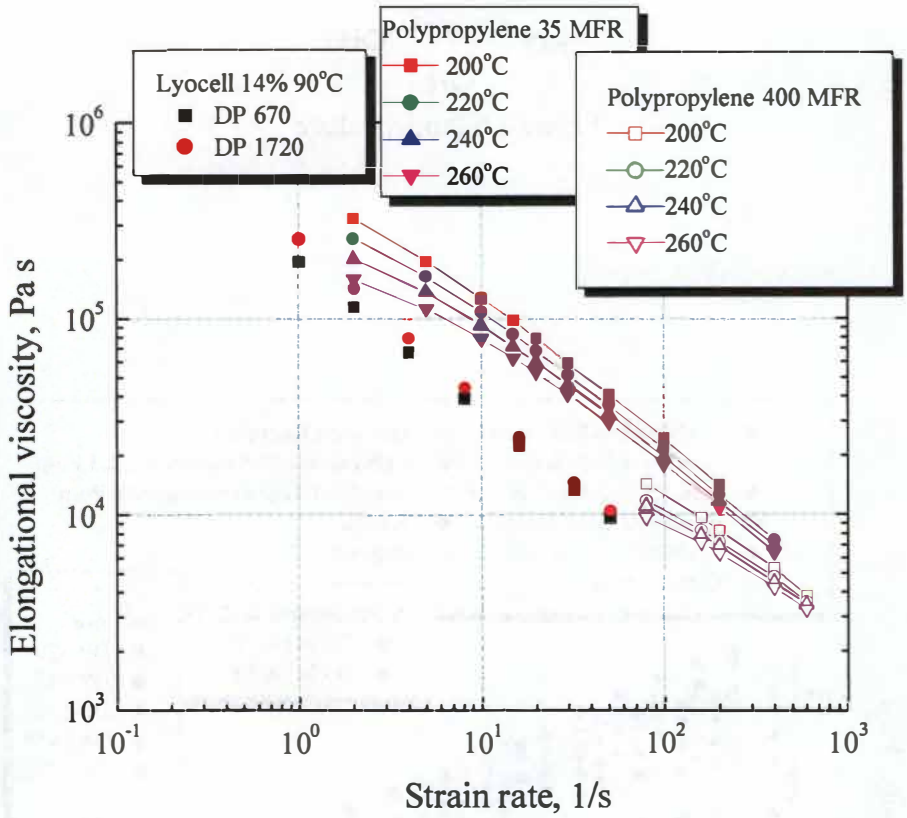

Figure 2.8. Comparative elongational viscosities

- Post treatment: washing, drying, finishing, cutting staple fibers
- NMMO recovery from the precipitation bath

The different parameters involved in fiber formation are air gap between the spinneret and the bath, temperature, humidity, solution water content, coagulation bath temperature, and cellulose concentration. These processing/material variables have been shown to determine the structure of the final fiber at the molecular level, thereby affecting the overall physical and mechanical properties [6, 49]. It is the exchange of solvent (NMMO) against the non-solvent (water) that dissolves the cellulose molecules and again helps in reforming the intra and intermolecular hydrogen bonds. There are other polar solvents such as alcohols and other solvents miscible with NMMO that could be used in place of water for removal of NMMO and coagulation of the fibers.

Most commercial lyocell spinning is done with 10-13 weight% NMMO monohydrate and 17-20 weight% of cellulose dissolving pulp. A number of researchers have demonstrated the dry-jet wet spinnability of NMMO and cellulose with different modifications involved [5 - 8, 50, 51].

Lyocell processing has advantages over the viscose process because of the nontoxic and biodegradable nature of NMMO, and its low environmental impact due to almost complete recovery and recycling (99.6%) of the solvent. The solvent can be recovered from the aqueous spinning bath by sorption onto a cation-exchange resin filtration system and water removal for concentration. The effect of NMMO on

the environment has been studied by developing and investigating various techniques such as degradation of NMMO by microorganisms, physical-chemical degradation involving TiO_2 photocatalytic degradation for morpholine, and ozonation of NMMO containing waste water [35, 52, 53].

2.2.4 RHEOLOGY

Rheology is the study of the flow and deformation of materials. It includes all aspects of the deformation of matter under the influence of imposed stress. Rheology gives information about how a polymer behaves internally under different conditions of force, temperature, and other influences. The rheological behavior of a polymer is influenced by temperature, rate of deformation, molecular weight, structure of the polymer, and various additives and fillers [54].

Rheology is an important parameter from the polymer processing point of view because it affects the stress levels a polymer will be subjected to in operations such as extrusion, fiber spinning, and film blowing. Rheological behavior influences the mechanical behavior of the polymeric material. Three types of flow exist in a flowing polymeric material: shear flow, elongational flow, and mixed flow. Measurements such as shear and elongational viscosity, storage modulus and loss modulus obtained during rheological study help in examining and understanding the interactions of different constituents in a multiphase mixture and their influence on the flow and other properties of such polymeric materials.

2.2.4.1 SHEAR FLOW

When a polymeric fluid is confined between two flat plates of area A separated by a distance D in a shear flow, all the motions are along one coordinate direction, the velocity varies along coordinate Z and the third direction is neutral. One of the instruments used for measuring shear viscosity is the Advanced Rheometric Expansion System (ARES) produced by TA instruments. It measures viscosity in torsional flow between a stationary and a rotating disk and can operate in a rotational or oscillatory mode as shown in Figure 2.9. Some of the variables involved in shear flow are [55]:

Shear Strain (γ)

When the upper plate is moved in the θ direction relative to the lower plate, the polymeric liquid is sheared with the amount of shear strain that is defined as:

$$\gamma = \tan\theta = \frac{S}{D}$$

where: S = Shear displacement

D = Distance between shearing surfaces

Shear Rate ($\dot{\gamma}$)

$$\dot{\gamma} = \frac{\text{RelativeVelocity}}{D}$$

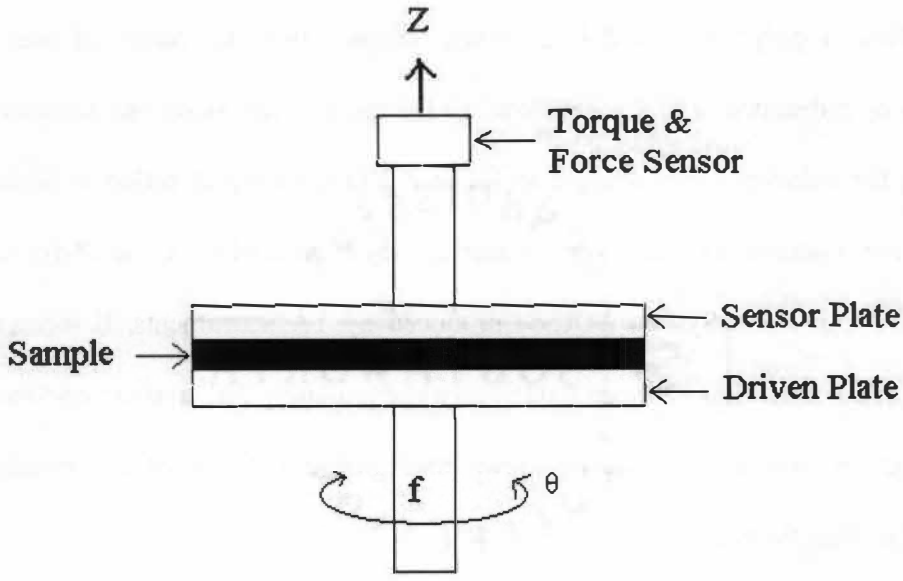

Figure 2.9. Parallel plate geometry

Shear Stress (τ)

$$\tau = \frac{F}{A}$$

where: F = Shear force ; A = Area

For a Newtonian fluid, shear stress is directly proportional to the shear rate where the constant of proportionality is viscosity (η). The rate of deformation is directly proportional to the applied stress. In general for polymeric fluids, with an increase in shear rate, the response becomes non-Newtonian and viscoelastic with shear viscosity of the polymer usually decreasing, exhibiting the behavior known as shear thinning. For a fluid in motion, with no slip at solid boundaries shear stresses are present.

2.2.4.2 ELONGATIONAL FLOW

When polymeric materials flow in channels or tubes with decreasing cross sectional areas, elongational viscosity comes into play. Elongational flow is the dominant mode of flow compared to shear flow when there is a sudden change of shape in a process like fiber spinning. For Newtonian liquids, the elongational viscosity is three times the shear viscosity.

The Advanced Capillary Extrusion Rheometer (ACER) with hyperbolic dies can be used for measuring the elongational viscosity of polymeric materials. A ram, operating at constant velocity is pushed through a uniform bored cylinder filled with

the polymer sample. The polymer is forced through a die of known shape and length. The volume of sample extruded per unit is expressed as [56]:

$$Q = \pi R^2 v$$

where: Q = Volume of sample extruded

R = Internal radius of cylinder, which is constant for a capillary die and for hyperbolic dies decreases as the die length increases

v = Liner velocity of ram

The apparent shear rate along the wall of the die is given by:

$$\dot{\gamma} = \frac{4Q}{\pi r^3}$$

where: $\dot{\gamma}$ = Apparent shear rate

r = Radius of the die

So for purely Newtonian behavior in a straight capillary die:

$$\dot{\gamma} = \frac{4R^2 v}{r^3}$$

A pressure transducer is located just above the die entrance to measure the pressure. At a constant sample velocity through the die, the apparent shear stress at the wall of the die is given as:

$$\tau_{\omega} = \frac{PR}{2L}$$

where: P = Pressure

L = Length of the die

With a change in the ram speed the resultant equilibrium pressure changes, making it possible to generate a flow curve of apparent elongational stress versus apparent strain rate. The apparent viscosity is given as:

$$\eta_a = \frac{\sigma_a}{\gamma_a}$$

where: η_a = Apparent viscosity

Another method was suggested for characterizing the elongational flow behavior of polymer melts using the hyperbolic dies on the ACER [57 - 59]. When capillary dies are replaced by hyperbolic dies, the effective elongational viscosity (η_{ef}) can be obtained by the following equation:

$$\eta_{ef} = \frac{\Delta P}{\dot{\varepsilon}\,\varepsilon_h} \qquad \varepsilon_h = 2\ln\left(\frac{R_o}{R_e}\right)$$

$$\dot{\varepsilon} = (v_0/L)(\exp\ \varepsilon_h - 1)$$

where $\dot{\varepsilon}$ = Elongational strain rate R_o = Entrance radius

R_e = Exit radius ΔP = Pressure difference

ε_h = Hencky strain , the natural logarithm of the area reduction

2.2.4.3 ORIENTATION

In fiber wet spinning the polymer is precipitated from solution by reaction and diffusion phenomena, leaving behind semi-solid strands of fibers which subsequently undergo drawing. The deformation of the material in the process takes place in two stages. As the extruded filament enters the coagulating bath from the spinneret hole, the filament coagulates and then is drawn out of the bath at a very low speed, lower than the final take-up velocity. The deformation taking place in the bath is not very effective since it has all been taken by the fluid portion of the filament before coagulation, the relaxation rates are very high, and the low deformation does not yield significant orientation in the filament. In the second stage molecular orientation is achieved by stretching and drawing. With increase in take-up velocity, orientation increases

In cases where the coagulation takes place by chemical reaction in the bath the stress developed is lower than when the operative mechanism is diffusion of the solvent out of the filament since the coagulation or gelling is faster than precipitation [59, 60]. The stress developed along the spinline in solution wet spinning is low compared to the stress levels in melt spinning and it is concentrated on the solidified skin; however it is still sufficient enough to produce permanent orientation of molecules [61]. The higher orientation in the skin has been confirmed by birefringence measurements. It has been suggested that orientation involves

deformation of solid and gel parts during the process instead of flow of fluid polymer solution as observed for melt spinning.

2.2.5 FIBER PROPERTIES

Lyocell properties are compared to those of other fibers in Table 2.2 [6 - 8]. Its specific advantages over other regenerated cellulosic fibers are [13, 51]:

- Higher modulus and orientation and lower elongation
- Higher knot and loop strength
- Better blending with other natural or manufactured fibers
- Better resistance to washing and drying
- Easier to spin to finer counts

Lyocell fibers have a tendency to fibrillate during wet processing especially under a mechanical stress which disrupts the fiber structure due to breaks or splitting of the single fiber in the longitudinal direction which leads to formation of fine fibrils that cling on the surface of the fiber giving a hairy feel and appearance to the fiber [5]. The fibers are highly crystalline but have weak lateral cohesion between the microfibers [6]. High bath temperature and post treatments such as bleaching, brushing, milling, grinding, sanding and sueding of the fibers increase fibrillation.

Fibrillation has both advantages and disadvantages. Where high surface is required for filtration efficiency and also for spun lace fabrics, it improves

Table 2.2 Fiber properties

Fiber Type	Cotton	Rayon[a]	Silk	Lyocell MB[b]	Lyocell (Dry jet wet)	Tencel Lyocell®
Typical Length (cm)	4	40	$>10^4$	Continuous		Variable
Typical Diameter (μm)	20	16	10	9-15		12
Tenacity (g/d)	2.5-3.0	0.7-3-2	2.8-5.2	2-3	37.5 (cN/tex)	4.5-5.0
Crystallinity Index	85%	35-40		67-73%	-	70-78%
Dry Elongation	10	20-25%		10%	14%	14-16%

a: by viscose process
b: DP 600 using lyocell process

entanglement and cohesion among the fibers compared to smooth fibers. It also gives smoother hand and appearance to lyocell fabrics. Drawbacks include abrasion marks and pilling formation during laundering. Excessive fine fibrillation can possibly give a snowy white frosty appearance to the finished fabric and also lead to small lint balls called pills.

Another problem associated with lyocell fibers is a lack of natural crimp like cotton which makes its processing difficult in the carding step due to insufficient separation among the fibers which further leads to poor blending with other fibers. An additional process called crimping is required in order to give crimp to the cellulose fibers. Also due to lack of crimp the fibers are very glossy which at times is undesirable.

2.2.6 APPLICATION

Areas of potential application of these fibers include hygiene and medical products due to their softness, high moisture absorption, breathability, high strength (dry/wet), and dimensional stability under wet conditions. Lyocell fabrics can also find a big share in the market of furnishing fabrics and in the apparel industry due to their good drapeability, luster, soft hand and versatile nature due to different surface finish, dyes and colors and textures. Lyocell fibers are also used in battery separators, air/gas/smoke/liquid filters, photographic papers, and tea bags. Lyocell's biodegradability and its processing involving fewer manufacturing steps compared to cotton spinning and weaving make it a strong contender in many of these markets.

Another growing area employing the use of lyocell fibers is spun lace nonwovens. Lyocell fibers have better performance in terms of bondability and strength compared to other types of cellulosic fibers, and less energy and pressure are required to form the webs. They also have a broader processing range in terms of basis weight, appearance and strength [51].

2.3 IONIC LIQUIDS

Ionic liquids (ILs) are a new class of compounds belonging to the family of molten salts. ILs consist of nitrogen containing organic cations combined with smaller inorganic anions. Cations found in common ILs are quaternary ammonium, immidazolium, or pyridinium. Anions may be Cl^-, Br^-, I^-, BF_4^-, triflate (trifluoromethanesulfonate) or others [62, 63]. The ILs are stable, nonvolatile and are liquid at room temperature, having melting temperatures less than 100°C.

ILs have been known to researchers since 1929 but it was not until 1992 that the first IL was prepared on a laboratory scale, with commercial production following in 1999 [64]. Some of the commercially existing ILs are [62]:

- 4-n-butyl-pyridiniumtetrafluoroborate [4-nBPPyr][BF_4]
- 1-n-butyl-3-imidazolium chloride [BMIM][Cl]
- 1-n-butyl-3-imidazolium bromide [BMIM][Br]
- 1-n-ethyl-3-methylimidazolium-bis(trifluoromethylsulfonyl)imide [EMIM][NTf_2]

- 1-n-butyl-2,3-dimethylimidazolium tetrafluoroborate [BMMIM][BF_4]
- 1-butyl-3-methylimidazolium chloride ([C_4MIM]Cl)

In the past few years there has been a growing interest in ILs for several reasons [62]:

- They are benign solvents with zero vapor pressure which makes them environmentally safe and results in their being labeled "green solvents".
- They are recyclable and therefore economical.
- They have a very wide liquidus range.
- They are polar in nature due to the coulomb forces acting between the ions, giving them the ability to selectively dissolve certain compounds such as cellulose.
- They can be used as catalysts.

Lack of available data and other resources for ILs in the literature however has been a barrier to realizing the full potential of these unique compounds. The concept of "green solvents" originated under the Environmental Protection Agency's (EPA) concept of "green chemistry" established 15 years ago. This initiative was designed to make solvents/chemicals which are ecofriendly and pollution free, require fewer reagents and less energy to produce, generate less waste, and are recyclable [63]. ILs have found potential applications in polymer processing and electrically conducting systems due to their ionic character (electrolytes in batteries

and photochemical devices), extraction and separation processes, organic synthesis, lubrication, thermofluids, and plasticizers [65, 66].

2.3.1 PROPERTIES

ILs have been used as solvents as well as catalysts due to their ability to be tailored for specific end uses [67 - 70]. In general they have no vapor pressure except for some choloroaluminate ILs (Al_2Cl_6). This means they do not exhibit a boiling point, critical pressure, heat of vaporization or flash point. Some anionic liquids though may burn when mixed with flammable substances [71]. The surface tension of ILs lies between that of other organic solvents and water.

ILs are more viscous than other molecular solvents. Dynamic viscosities from 10-1000 cP at room temperature have been reported [67]. They are known to be thermally stable up to 200°C compared to other molecular solvents. Other common properties are:

- Most of the ILs are noncorrosive or less corrosive and safe except for some (cholroaluminates) compared to conventional high melting salts [64, 67, 72].
- ILs have no sharp melting point due to their supercooling nature which makes them liquidus over a wide range of temperature. The lower liquidus range is taken as the melting point and is usually lower than 100°C [64].
- ILs have a very low glass transition temperature <50°C with a very high viscosity which makes them unsuitable for sub-zero chemical reactions [67].

- ILs are less toxic than organic solvents; however there is a lack of sufficient literature on their overall toxicity. Some of the work done in past reports the toxicity level of some of the most toxic ILs to be the same as that of some of the organic solvents: methanol, acetone, and acetonitrile [67, 73].
- Some of the ILs are highly hygroscopic in nature ([C_4MIM]Cl).

2.3.2 DISSOLUTION MECHANISM

As mentioned earlier ILs can act as solvents for certain compounds and cellulose is one such biopolymer that can be dissolved in [C_4MIM]Cl. There is a growing interest in cellulose and ILs due to their ecofriendly properties; however this system has not been thoroughly researched. So far various ILs having different anions have been tested and studied for cellulose dissolution and [C_4MIM]Cl showed the best results in terms of time taken to dissolve the cellulose. This is due to its stronger hydrogen bond acceptor anion, i.e. chlorine [74]. It also been shown that cellulose dissolution is decreased in the presence of water because the water molecules compete with the IL for the cellulose hydrogen bonding sites.

The dissolution chemistry of cellulose in [C_4MIM]Cl is similar to that of lyocell (NMMO•H_2O/cellulose). The solvent breaks the hydrogen bonds between the cellulose hydroxyls and forms hydrogen bonds itself, moving the cellulose chains apart. The chloride ion in [C_4MIM]Cl disrupts the intramolecular hydrogen bonding among the hydroxyl groups in cellulose leading to dissolution of cellulose in the IL.

For both systems another solvent such as water or ethanol is needed to precipitate the cellulose.

The IL should be recoverable from the precipitation bath just like NMMO due the fact that it has no vapor pressure and there is no loss during processes such as fiber spinning. The IL recovery is still at the experimental stage where researchers have tried various techniques to recover the solutes after the processing. Some of the techniques explored so far are supercritical carbon dioxide extraction, liquid-liquid extraction using aqueous systems, crown ether extraction, prevaporation, and membrane techniques [75]. However these methods are not free of drawbacks. Supercritical carbon dioxide extraction, for example, is an efficient technique applicable to wide range of ILs but it requires high precision and is technically very complex to perform [75, 76].

2.3.3 SYNTHESIS

The IL [C_4MIM]Cl can be synthesized by reacting 1-methyl imidazole with alkyl halide in an ultrasonic bath as shown in Figure 2.10 [65]. Sonochemical preparation has proven to be more efficient in terms of energy and amount of reactants required compared to the conventional method, which is energy intensive because of the longer heating time and waste due to the excess of reactants. Also in

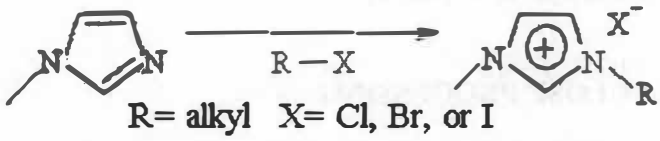

Figure 2.10. 1-Alkyl-3-imidazolium halide synthesis

the conventional method, prolonged exposure to heat results in overheating of the reactants and a colored solvent product.

2.3.4 IL/CELLULOSE PROCESSING

Theoretically IL/cellulose processing should follow the same guidelines as the lyocell process. So far very little work has been done by researchers in the processing of ILs with cellulose. Laboratory scale spinning has been demonstrated for different concentrations of cellulose [77]. Fibers were spun using different cellulose sources and $[C_4MIM]Cl$ as solvent. Tenacity of the fibers ranged from 1.89-4.41 g/den and elongations were 3.8-30.9% [77].

2.4 ELECTROSPINNING

2.4.1 INTRODUCTION

Electrospinning is a technique where spinning of fibers is done under an electrostatic force field applied by a high voltage DC source. It is known to produce nanofibers having a diameter less than one micron [78].

Electrospinning has been known to researchers since the 1930s. However it was only after the work of Formhals that the potential of the electrospinning process was recognized due to its simplicity and the advantages it offers [79, 80]. Since then jet formation during the electrospinning process has been studied in more depth by other scientists. The concept of the "Taylor Cone" was formulated by Taylor, who discovered that the angle of the polymer droplet formed at the tip of the spinneret

should be at least 49.3 degrees in order to balance the electrostatic force and the surface tension of the polymer [81, 82]. The pioneering work of Doshi and Reneker [78] broadened interest in this emerging field. They demonstrated the spinning of various polymers in different solvents and studied the fundamentals more extensively.

Various polymers have been successfully electrospun in a number of solvents and their details can be found in the literature [81]:

- polyethylene terephthalate in a mixture of dichloromethane and trifluoroacetic acid
- polyether urethane in dimethyl acetamide
- polystyrene in tetrahydrofuran
- polyethylene oxide in isopropyl alcohol
- polycarbonate in dimethyl formamide and tetrahydrofuran
- cellulose acetate in acetone

The main advantage of electrospun nanofibers is the high surface area per unit mass due to the ultra fine fibers and small pores between fibers (Figure 2.11) [83]. The electrospinning process has been efficient in making fibers in the nano range (100 nm-500 nm). These have found applications in filtration, medical fabrics, wipes, battery separators, energy storage, protective clothing, catalyst substrates, adsorbent materials, optical fibers, drug delivery systems, tissue scaffolds,

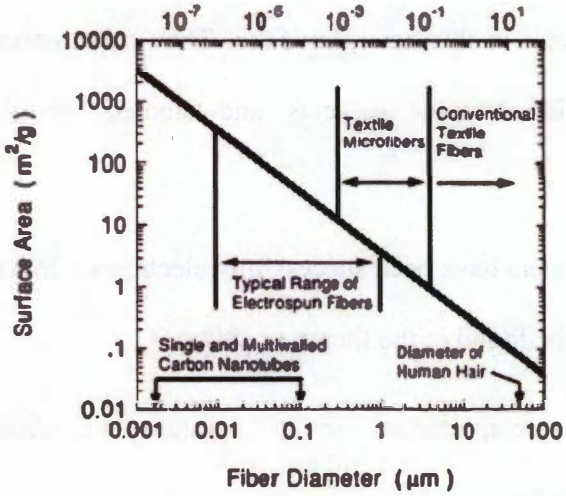

Figure 2.11 Relationship between fiber diameter and surface area of nylon 6,6 fiber [83]

reinforcing material for composites, nanocomposite smart textiles, and others [78, 81, 84- 86].

2.4.2 PRINCIPLE

A laboratory scale setup for electrospinning basically consists of a DC source, a syringe with a specific needle size, a metering device to control the throughput of the polymer melt, and a collector. A schematic of one type laboratory scale setup with a horizontal syringe and metering pump is shown in Figure 2.12. An alternate configuration uses a vertical arrangement of the syringe and the needle resulting in gravity feed of the spinning solution. It may be used with or without metering pump [87]. In conventional spinning, the fiber is subjected to rheological forces, aerodynamic forces, gravitational forces, and tensile forces generated due to the positive drawing mechanism. In electrospinning however, the electrostatic and mechanical forces are the primary mechanisms of the system.

The spinneret is maintained at a positive or negative charge by a DC power supply and the collector is grounded (or vice versa). This high potential difference between the two results in formation of a conical region, with its apex at the tip of the spinneret within this conical region fiber streams separate and whip. The high electric field overcomes the critical surface tension force in the polymer droplet, forming these streams of several jets [82]. As the streams travel to the collector the solvent evaporates, thereby drying the jets and leading to coagulation of the jets as small or nanofiber streams. The collector can either be a fixed plate or can be a

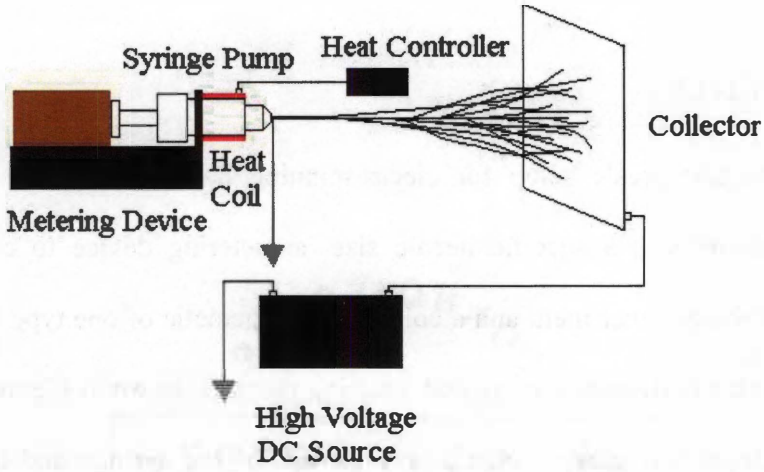

Figure 2.12 Schematic of laboratory scale electrospinning setup

rotating roller [88]. There have been trials done with the collector submerged in a grounded water bath which affects the morphology and fiber properties [89, 90].

2.4.3 ORIENTATION

The nonwovens formed by electrospinning are randomly oriented because of the chaotic oscillating electrospinning jets that give little control over the forces involved in the fiber orientation and crystallization. The variables responsible for controlling the molecular orientation of the fiber are applied electric field, solution concentration, type of solvent and type of polymer, conductivity of the polymer fluid, viscosity of the solution, and throughput/feed rate of the polymer.

In an electrospinning process the spinning jets experience large draw ratios due to the high applied voltage and electric fields, and hence the resulting fibers would be expected to have some amount of orientation. If there is no restraining force or fibers are not solidified then orientation developed during the electrospinning process may therefore be lost due to rearrangement of the polymer chains. For moving collectors the fibers can be stretched further, resulting in increased drawing and better alignment of the fibers and more permanent orientation in the fibers [82, 73]. Molecular orientation along the fiber axis can also be imparted as the fiber travels from the capillary exit to the collector because of the strain it experiences in the jet. With increases in applied voltage and electric field the fiber diameter has been shown to decrease due to higher pulling and stretching forces over

the polymer jet, which in turn can be related to higher molecular orientation in the fiber [91].

2.4.3.1 PROCESS VARIABLES

Just like any spinning or polymer processing operation, electrospinning has certain process/material variables which control the overall surface and structural properties of the fibers/webs obtained. Different variables involved are solution viscosity, solvent vapor pressure and conductivity, surface tension, applied voltage, polymer throughput, and spinneret to collector distance. Extensive work has been done by Theoran *et al* to study and optimize the governing process and material variables [92].

Fiber diameter of the jet is dependent on the voltage applied, going to a minimum value at a certain maximum voltage; beyond that maximum value the fiber diameter increases [93]. Solvent conductivity also affects the fiber diameter and the stability of jet streams [94].

The distance between the spinneret and the collector influences the fiber morphology as it controls the evaporation rate, deposition time, and the instability or the whipping interval [81, 95]. The polymer throughput affects the fiber/web structure by controlling the jet velocity and the material transfer rate. In early work, increased throughput was shown to increase the fiber diameter and the pore size [95, 96].

Having the right viscosity of the solvent is also important as a lower viscosity results in droplet formation on the collector making it impossible to collect fibers. Higher viscosity solutions though can either result in very thin fibers or a poor fiber/mat due to discontinuous flow caused by the intense cohesiveness of the solution [97, 98]. Fiber diameter, droplet shape, and jet trajectory have been shown to be affected by the solution viscosity [84].

2.4.4 CELLULOSE ELECTROSPINNING

Cellulose was electrospun for the first time as cellulose acetate in 1934 by Formhals using acetone as solvent. This system has since been used by other researchers to electrospin cellulose fibers [79, 81]. There has been work reported in the past dealing with electrospinning: a) cellulose acetate membranes in a solvent of acetone, acetic acid and dimethylacetamide [85]; b) ethyl cellulose in tetrahydrofuran or dimethylacetamide [86]; c) cellulose in lithium chloride, N, N-dimethylacetamide, or NMMO) [77,87]. The effects of different concentrations and processing conditions on the fiber structure and morphology have also been studied [90 , 98 - 100].

2.5 MELT BLOWING

2.5.1 INTODUCTION TO MELT BLOWING PROCESS

Melt blowing (MB) is a process for making nonwoven fabrics in which a molten polymer is extruded through a multiple hole die and the fibers are attenuated

by high velocity hot air streams. The solidified, very fine fibers are collected on a moving belt, forming a nonwoven web. A schematic for the MB process is shown in Figure 2.13. Melt blowing has been restricted to thermoplastic polymers that form fibers from the polymer melt because of ease of processing and the lack of a vapor pressure. The process has therefore not been amenable to dry or wet spinning where volatile, and often hazardous, species are generated when the solvent is removed from the fibers.

The solvent in the lyocell process however has essentially no vapor pressure and a low melting point (~90°C), and therefore melt blowing cellulosic nonwovens from lyocell solutions is feasible. Luo et al. demonstrated this in a series of patents issued in recent years [6 - 8].

Combining the advantages of the regenerated cellulosic fiber lyocell with the economical fabric forming process of MB, offers potential new product applications for both technologies. These include hygiene and medical products where softness, high moisture absorption, breathability, strength, and dimensional stability are desired. Cellulose, as an absorptive and reactive polymer, would provide properties not currently available in MB nonwovens composed of thermoplastic polymers. The fibers in MB webs are very fine, in the range of microfibers, contributing a high surface area to the webs which are often used in filters. Absorption and retention are affected not only by the web structure, but also

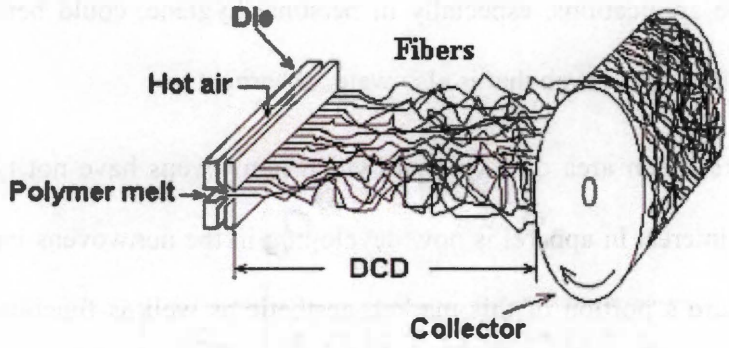

Figure 2.13 Schematic for MB process (Courtesy: Dr. Simioan Petrovan)

by the chemical nature of the polymer. Cellulose in such a filter medium provides another dimension to the aim of maximizing filtration efficiency. Further, many kinds of wipe applications, especially in personal hygiene, could benefit from the softness of a microfiber web that is also water absorbent.

Apparel is an area of textiles in which nonwovens have not typically been seen. A new interest in apparel is now developing in the nonwovens industry and in order to capture a portion of this market, aesthetic as well as functional properties must be considered [101]. The regenerated cellulosic fibers, rayon, acetate, and triacetate, have long been known for their aesthetic qualities, particularly drapeability, and now lyocell has joined their ranks. Lyocell nonwovens may offer designers and manufacturers alternative and cost effective materials for their product lines.

2.5.2 ELEMENTS OF MELT BLOWING PROCESS

A typical MB process consists of the following elements: extruder, metering pump, die assembly, web formation, and winding.

2.5.2.1 EXTRUDER

The extruder is one of the important elements in many polymer processing operations. It consists of a heated barrel with a rotating screw inside. Its main function is to melt the polymer pellets or granules and feed them to the next step/element. The forward movement of the pellets in the extruder is along the hot

walls of the barrel between the flights of the screw. The melting of the pellets in the extruder is due to the heat and friction of the viscous flow and the mechanical action between the screw and the walls of the barrel. The screw has different heating zones depending upon the length of the screw. Extruders are classified based on the number of screws: single-screw extruder or twin-screw extruder [102].

Any extruder can be divided in to three different zones [103]:

i) Feed Zone: In the feed zone the polymer pellets are preheated and pushed to the next zone.

ii) Transition Zone: The transition zone has a decreasing depth channel in order to compress and homogenize the melted polymer.

iii) Metering Zone: This is the last zone in the extruder whose main purpose is to generate maximum pressure in order to pump the molten polymer in the forward direction. At this point the breaker plate controls the pressure generated with a screen pack placed near to the screw discharge. The breaker plate also filters out any impurities such as dirt, foreign particle metal particles and melted polymer lumps.

2.5.2.1.1 TWIN SCREW EXTRUDER

A twin-screw extruder is similar to a single screw extruder in its construction except that it has two screws in the barrel instead of one screw. The twin-screw extruder is particularly useful in processes requiring mixing of different materials right before extrusion [102]. Unlike the single screw, the twin-screw extruder is

usually starve fed so as to have a throughput independent of the screw speed due to the fact that flood feeding might result in very high pressure leading to the failure of the thrust bearing. Since good mixing generally occurs in a twin-screw extruder, the polymer melt mixes well and efficiently and can be conveyed in a shorter machine length compared to that of single-screw extruder.

The two screws can either be co-rotating (turning in the same direction) or counter-rotating (turning in the opposite direction). Co-rotating screws are used when homogenous compounding is required. Some of the advantages offered by co-rotating screws are:

- If the screws are intermeshing, screws clean each other by a self wiping action due to their same direction of rotation
- Offers high screw speeds and higher throughput
- Less wear and tear on the screws and the barrel

Counter-rotating screws are often preferred when compounding and extrusion are required simultaneously. They offer the advantages of:

- Positive feeding and conveying
- Uniform polymer residence time
- Uniform material temperature control

However the counter-rotating screws have drawbacks of having air trapped while taking in polymer, high pressure in the melt, low maximum screw speed and low throughput, unlike the co-rotating screws.

2.5.2.1.2 VENTED EXTRUSION

In vented extrusion there is a provision for a vent in the extruder barrel for the volatiles to escape during the extrusion process. The volatiles can be water vapor, degradation reaction products or some evaporative solvent used as a compounding ingredient which if not removed would degrade the end product. The vent is usually located at the point where the melt is decompressed by reducing the root screw diameter. When the vent is open, in order to avoid the escape of the polymer melt there is often an additional component called a dam or torpedo built in right before the vent.

2.5.2.2 GEAR PUMP

The gear pump is a set of two intermeshing, positively driven and counter rotating toothed gears. It provides a constant volume of melted polymer to the die assembly for uniform delivery under various operating conditions.

2.5.2.3 DIE ASSEMBLY

The die assembly has four different components:

i) Polymer Feed Distribution: This component uses a coat hanger shaped feed distribution to provide even polymer flow and residence time across the full width of the die.

ii) Die Nosepiece: It is a tapered piece of metal generally having several hundred holes in a row across its width through which the polymer melt is extruded in order to make filament strands. These are subsequently attenuated by hot air to make fibers as shown in Figure 2.14 [103].

iii) Air Manifolds: The function of the manifold is to supply high velocity hot air through the slots on each side of the die nosepiece.

iv) Air Knives: These are die components that can be moved to control the air gap on each side of the die. This in turn determines the volume of air that flows concurrently with the extruded fibers.

2.5.2.4 WEB FORMING

The filament strands are attenuated to microfibers when they exit the die holes by means of high velocity hot air and are laid randomly on the surface of the collector in the form of a nonwoven web. The nonwoven web formed is a physically bonded structure containing entangled and partially fused fibers. Cooling and solidification of the fibers are achieved with the help of surrounding cold air. The web can be formed in two ways depending on whether the collector is horizontal or vertical.

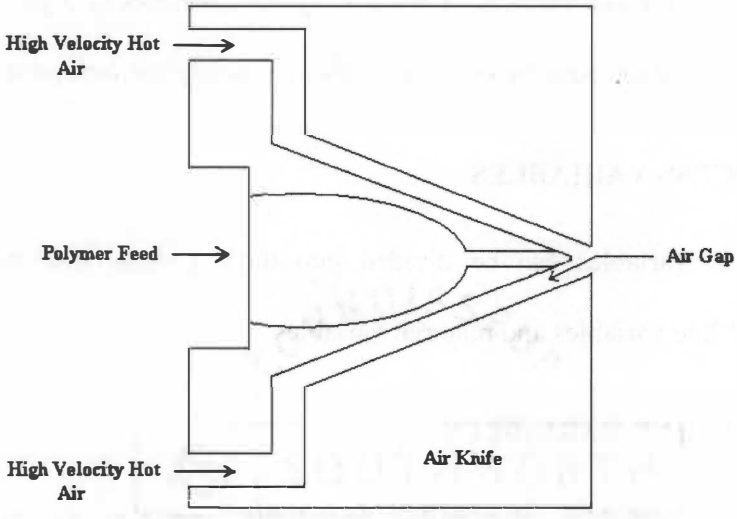

Figure 2.14 Schematic showing the air flow through the die assembly

2.5.2.5 WINDING

Winding, the last element of the MB system, consists of a positively driven mechanism serving the purpose of continuously collecting the web produced.

2.5.3 PROCESS VARIABLES

Process variables can be divided into three groups: machine/operational variables, off-line variables and material variables.

2.5.3.1 MACHINE VARIABLES

Machine variables, also called operational variables, are related to the machine and can be changed while the equipment is being operated. These variables include air temperature, polymer/die temperature, die to collector distance (DCD), collector speed, polymer throughput and air throughput. All of these affect the final properties of the nonwoven web.

a) Polymer Throughput and Air Flow: Both polymer throughput and air flow rate influence the final fiber diameter, fiber entanglement, basis weight and the attenuating zone.

b) Polymer/Die and Air Temperature: These variables combined with air flow rate affect the uniformity, shot formation (globules of nonfibrous polymer larger in diameter than fibers in the webs), rope and fly formation, fabric appearance and feel (soft or stiff).

c) Die to Collector Distance: This affects the openness of the fabric, thermal bonding among the fibers, and basis weight.

2.5.3.2 OFF-LINE VARIABLES

Off-line variables are fixed during a process run and can only be changed when the machine is not in operation. These variables are air gap, air angle, die setback, and die hole size.

a) Die Hole Size: Die hole size along with die set back affects the fiber size.

b) Air Gap: It affects the degree of fiber breakage by controlling the air exit pressure.

c) Air Angle: It controls the nature of air flow, i.e. as the air angle approaches 90° it results in a high degree of fiber separation or turbulence that leads to random fiber distribution. At an angle of 30°, roped or parallel fibers deposited as loosely coiled bundles of fibers are generated. This structure is undesirable. At angles greater than 30°, attenuation as well as breakage of fibers occurs.

2.5.3.3 MATERIAL VARIABLES

Material variables include polymer type, molecular weight, molecular weight distribution, melt viscosity, polymer additives, and polymer pellet size (powdered or granular). The MB process is amenable to a wide range of polymers in terms of viscosities and blends.

2.5.4 ORIENTATION

In the MB process the fiber orientation is defined at two different levels: one is at the molecular level i.e. molecular orientation in the fiber and the other is the orientation of the fibers in the nonwoven web. Melt throughput, extrusion temperature, and molecular weight of the polymer affect the molecular orientation prior to exiting the die. After the polymer exits the die in form of filaments, the process variables affecting molecular orientation are air temperature, air velocity, and die-to-collector-distance (DCD).

The MB process is similar to the conventional melt spinning process except for one major difference: instead of drawing the freshly formed fibers between godet rollers operating at different speeds, streams of hot air are used to attenuate the fibers. Since the air is approximately the same temperature as that of the polymer, it provides a forwarding force to the fibers preventing them from solidifying immediately. The air drag experienced in this environment is of primary importance in orienting the fibers. Beyond a certain distance from the die the fibers cannot be attenuated any further as they have solidified. The increase in orientation beyond a critical elongational deformation due to structural changes in the polymer melt influences solidification "freezing" [104]. Most of the molecular orientation takes place before the freeze point and later there is a small increase in the molecular orientation due to elongation of fibers in the entangled web structure.

As the fibers move away from the die, entanglement and contact with adjacent fibers result in a stretching force on the fibers and increased molecular orientation. This has been confirmed by birefringence measurement (Figure 2.15) [105]. Molecular orientation begins only after attenuation has occurred in almost all the fibers and orientation continues to increase (although it might be a small increase) all the way to the collector since the fibers do get elongated in the later stage as stated above. As the air velocity increases, the air drag force (due to greater difference in the air velocity and fiber velocity) further stretches the fibers resulting in higher spinline stress and increased molecular orientation.

Orientation of the fibers in the nonwoven web is defined as the angle between the fiber path and an arbitrary web direction which is usually the machine direction (MD), that in which the web is moving. The orientation is mainly affected by the die-to-collector distance (DCD). At lower DCDs, fibers are more oriented towards the MD due to the increased tendency of the fibers to blow over the collector, whereas the reverse is the true in the case of higher DCDs [106].

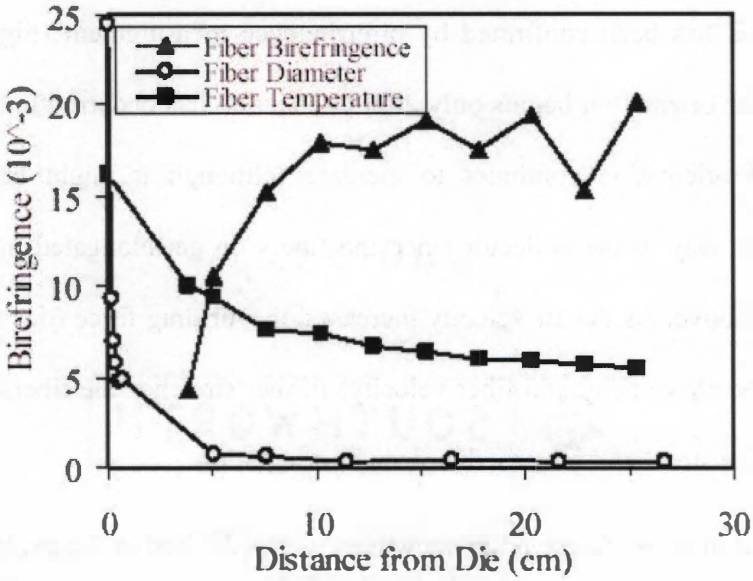

Figure 2.15 Birefringence of fibers in relation to distance from the die [105]

Chapter 3 Procedures

3.1 SAMPLE PREPARATION

3.1.1 PREPARATION OF LYOCELL SOLUTIONS

Commercially NMMO was purchased as 50/50 weight % NMMO/water from Huntsman Corporation. Cellulose, DP 670, dissolving pulp was supplied by Buckeye Technologies, Memphis. Samples were ground well and dried at 90-95°C for 3-4 hours in vacuum oven. In order to dissolve cellulose in NMMO, monohydrate form (NMMO•H_2O) is needed. There are two ways in which NMMO/cellulose solutions can be prepared

- The first method is mixing the cellulose and propyl gallate (1% by weight of pulp) with NMMO having a hydration number ≥ 1.65. The solution is heated until the excess water evaporates and the hydration number drops to one. This method is efficient in giving homogeneous solution of NMMO•H_2O/Cellulose but it results in degradation of the solution due to the long heating time at elevated temperatures to drive off the excess water.
- A second method creates the monohydrate first by heating NMMO/H_2O to evaporate the water in a mixer. This method is efficient in preventing the degradation of the solution however it can give a nonhomogeneous solution due to poor diffusivity of the NMMO•H_2O into the cellulose at higher

concentrations. This drawback can be overcome by mixing at higher speeds for longer times depending op the concentration of the cellulose.

The second method was used in this work to prepare the NMMO/cellulose solution. Initially NMMO/H_2O (50 wt%/50wt %) was taken and condensed to NMMO monohydrate (NMMO•H_2O) in a rotary evaporator under vacuum which was heated in a silicon oil bath until the monohydrate was achieved (87% NMMO). The molecular weight of NMMO is 117 and that of NMMO•H_2O is 135. The NMMO monohydrate was sealed in a bag. Later this NMMO•H_2O and pulp were added in the twin screw extruder in the required proportion for compounding/mixing and the solution was extruded out of a MB die.

3.1.2 PREPARATION OF IL/CELLULOSE SOLUTION

The IL, 1-butyl-3-methylimidazolium chloride ([C_4mim]Cl), was purchased from Fluka Chemie in powder form. Solutions of two different concentrations of cellulose (3% and 7%) in [C_4mim]Cl were prepared. These concentrations were selected based on solution viscosities studied previously. Preliminary work had shown that the viscosities of 3% and 7% solutions were similar to typical solutions used in electorspinning [92]. To prepare the solutions, sample bottles containing 15 mg of the IL were placed in an oven at 90°C until the solution melted. Previously dried dissolving pulp was added to achieve the selected weight concentration, and the sample bottles were returned to the oven. The solutions were stirred with a spatula every 10-15 minutes until all the cellulose was dissolved and a clear solution

was obtained. was obtained It is important to dissolve the pulp thoroughly prior to fiber spinning and ensure that the solution is clear and free from any residual and undissolved fibers which in the later stage can lead to fiber breaks or discontinuity in the spinning line and clogging of the die hole in spinning as well as in MB.

3.2 LYOCELL MELTBLOWING

There are various operating variables that can be studied in a MB process. The objectives of this research were to evaluate the MB capability of lyocell solutions and to measure the properties of MB cellulosic nonwovens. Runs were made at the Textiles and Nonwovens Development Center (TANDEC) at the University of Tennessee on a modified 6 inch MB system with a Leistritz twin screw extruder as shown in Figure 3.1.Various MB nonwoven samples were made for different combinations of the process conditions on a this MB pilot line at TANDEC. The die configuration used for this setup was as follows:

Nozzle Diameter = 0.254 mm Air gap = 0.762 mm

Set back = -0.762 mm Number of holes = 150

Different settings were used for the different extruder and die temperatures as shown in Table 3.1. Different settings were tried for air and DCD in order to generate good MB webs. Once the web was collected it was kept in a water coagulation bath.

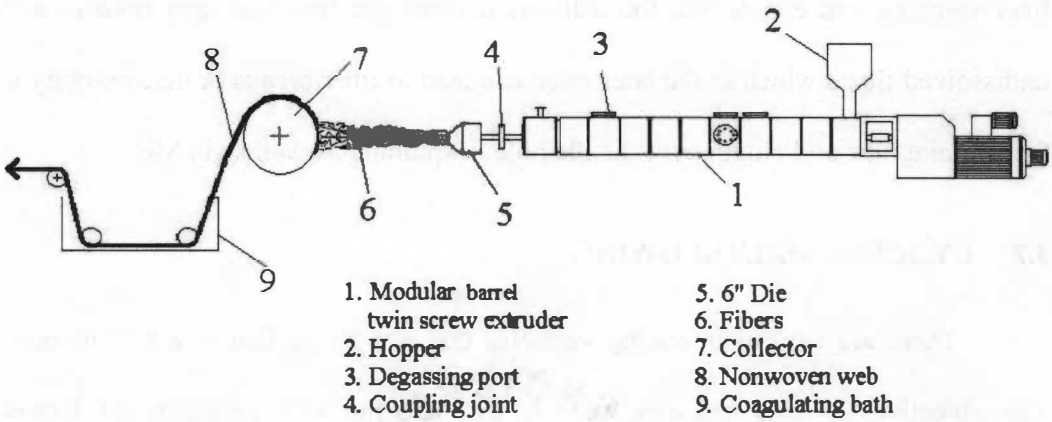

Figure 3.1 Twin screw MB system

Table 3.1 Different processing conditions

Sample ID	Neck Temp(°C)	Die temperature profile (°C)				Air temp. (°C)	DCD (cm)
		Bottom	Top				
May 2004 #2	97	97	97	97	97	97	91.44
May 2004 #3	100	100	100	100	100	100	91.44
May 2004 #4	113	113	113	113	113	113	60.96

3.3 ELECTROSPINNING OF IL/CELLULOSE

A laboratory scale setup as shown in Figure 2.12 and Figure 3.2 was used. A glass syringe with a 10 mL capacity and needles with two different diameters (0.41 and 0.91 mm) were used. The syringe was filled with the cellulose solution and heated in an oven set at the run temperatures (95 and 100°C) for an hour to thermally equilibrate. The syringe was then removed from the oven and placed in the heating pad for 30 minutes to ensure a thermally stable system.

3.4 ACER ASSISTED SPINNING OF IL/CELLULOSE

The ACER with hyperbolic dies can be used as a fiber spinning setup due to induced elongational flow which reduces molecular relaxation at the spinneret producing highly oriented and crystalline cellulose fibers. This instrument also gives a precise control of throughput and temperature. The schematic of an ACER assisted spinning setup is shown in Figure 3.3. It consists of a barrel with a ram that forces the molten polymer or polymer solution through a hyperbolically converging die. The molecular chains are in a highly coiled state distributed randomly in the space and are also entangled with adjacent molecular chains. As the molten polymer is forced through an orifice with a gradually decreasing diameter (such as in the hyperbolic converging die) the polymer chains realign, uncoil and change their

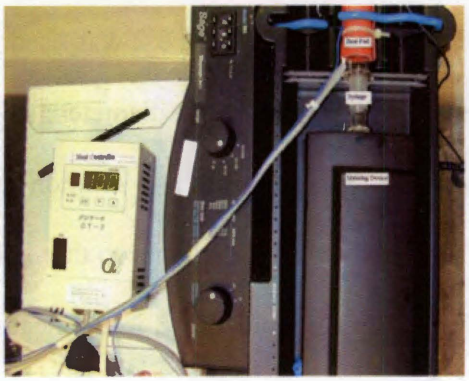

(a)

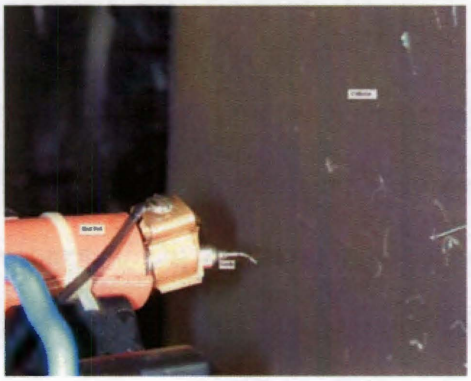

(b)

(c)

Figure 3.2.Electrospinning setup

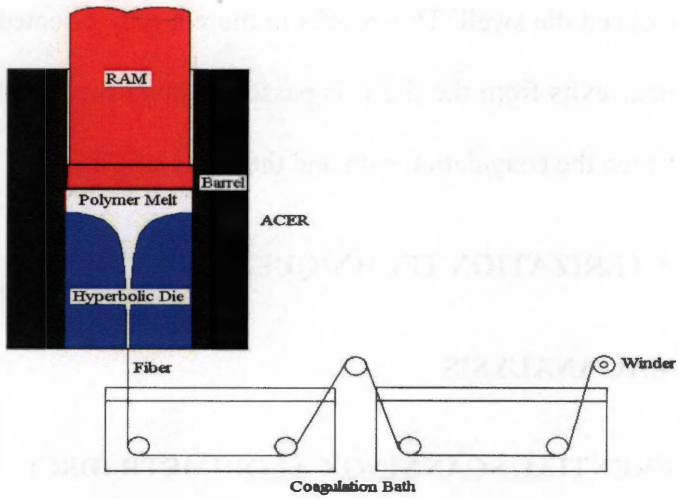

Figure 3.3 Schematic of a ACER assisted spinning setup

shape (Figure 3.4). This reduces their tendency to relax at the spinneret thus exhibiting the reduced die swell. This results in more highly oriented and crystalline fibers. As the fiber exits from the die it is passed through the coagulation bath and the distance between the coagulation bath and the die is adjustable.

3.5 CHARACTERIZATION TECHNIQUES

3.5.1 THERMAL ANALYSIS

3.5.1.1 DIFFERENTIAL SCANNING CALORIMETR (DSC)

The melting transition of the solvents and the solutions were determined on a Perkin Elmer Pyris 1 differential scanning calorimeter. The samples were held for one minute at 30°C and later heated at a rate of 5 and 10°C per minute up to 120°C. The cooling curves were obtained at a rate of 5°C per minute. All the samples were prepared in an enclosed nitrogen bag so as to avoid moisture absorption. One set was prepared by freezing in the liquid nitrogen for an hour.

3.5.1.2 THERMOGRAVIMETRIC ANALYSIS (TGA)

The degradation behavior of the solvents and the solutions were studied using a Mettler Toledo TGA/STDA 851^{e} setup. Samples were held for five minutes at the starting temperature (50°C) and then were heated at a rate of 20°C per minute up to 800°C

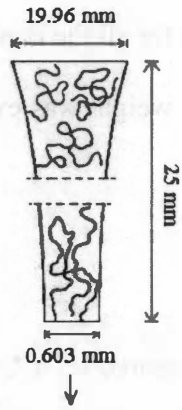

Figure 3.4 Schematic of orientation occurring in hyperbolic die [61]

3.5.2 BASIS WEIGHT

Basis weight was measured for all the nonwoven samples by weighing a 50.8 x 50.8 mm^2 sample size. The basis weight was expressed as grams per square meter (g/m^2), gsm.

3.5.3 TENSILE STRENGTH

Tensile properties were measured on a United Model SSTM-1-E-PC tensile tester and Instron setup. For a MB nonwoven web a sample with an area 50.8 x 152.4 mm^2 was tested. For fibers, the fiber bundle strength for an average of fifty fibers was tested for one inch gauge length.

3.5.4 THICKNESS

Thickness of the nonwoven webs was measured on a TMI Model 49-70 mm at a pressure of 4.14 ± 0.21 kPa. The dimension of the circular presser foot is 25.4 ± 0.02 mm diameter and that of anvil is 38 mm. This test was performed on the MB nonwovens webs (ASTM Standard D5729) [108].

3.5.5 ABSORBENCY

Absorption is the liquid uptake of the fibers whereas wicking is the liquid uptake by capillaries formed by fibers. The ATS-600 is a tabletop optical absorbency testing system designed for measuring absorption and desorption rates along with capacity measurements based on time and the amount of fluid displaced from the

fluid reservoir. During sample testing the optical sensor maintains a constant fluid level at a preset differential head. A programmable pulse introduces fluid to the sample allowing absorption at zero pressure. The different components of the ATS-600 are:

1. Syringe Assembly: The function of the syringe is to control fluid discharge. The fluid volume and weight are monitored by rotating the motor where one step is equivalent to 1.8 degrees of rotation. The syringe is connected to the main fluid reservoir and to the opto-detector via a three way valve.

2. Opto-Detector Assembly: It is a combination of an opto-detector and a small reservoir of fluid. The opto-detector works by sensing the height of the fluid in the column above the reservoir. The reservoir level is maintained by the stepping motor which adds or removes water thereby maintaining a constant preset head level on the sample during the test.

3. Test Table Platform: This holds the sample and can be set to different heights. It is connected to the opto-detector fluid syringe by silicone tubing. It uses an optional directional flow plate which gives the directional flow rate measurements. It consists of eight evenly spaced electrodes at every 45 degrees in a 20 mm radius circle around the center point-source. These electrodes facilitate the MD/CD measurement depending on time taken by the fluid to reach each of them.

There are two settings under which the ATS-600 can be run: 1) a timed run, where the test is run for a fixed time within the instrumental range of 1-3200 seconds, by plotting amount of liquid absorbed versus the time of the test; 2) a slope run, where the test runs until absorption reaches a desired rate. The slope run will generate an absorption curve [109]. All tests were run for at least 400 seconds in order to ensure that absorption had tapered off, and the differential fluid head was set approximately at zero [110, 111].

3.5.6 PORE SIZE

Pore size and distribution were determined using a PMI Capillary Flow Porometer Model CFP-1100-AEX. The instrument was operated in the dry-up/wet-up mode in which the dry phase was run before the wet phase. The sample was placed in the sample chamber, the air pressure through the system and the air flow rate through the sample were increased and data points recorded at each equilibrium point. With increasing air pressure, the smaller pores start to open and when either maximum flow rate of pressure or maximum pressure is reached the measurement stops [112]. The mean flow pore size is calculated using the equation given below for a pressure value at which wet flow is one half the dry flow. The bubble point test gives the maximum pore size on a nonwoven web. The maximum pore size is given as [113]:

$$d = C\,\tau/p$$

Where d: Maximum pore diameter (μm)

τ : Surface tension of liquid (dynes/cm)

p: Differential pressure

C: Constant 2860 when p is in PA

1.15 when p is in cm Hg

0.415 when p is in psi

3.5.7 CONTACT ANGLE

Contact angle, an indication of material wettability, was measured on a Kruss Processor Tensiometer – K14 using the Wilhelmy method (Figure 3.5) [114 - 117]. The sample dimensions used were 6 x 1 mm^2 for all the runs. Once the sample was cut it was adhered to the sample probe using double sided tape and hooked up on the microbalance.

3.5.8 SCANNING ELECTRON MICROSCPE (SEM)

The webs and fibers were examined under a Leo 1525 SEM. The emission voltage was varied between 1-3 KV to avoid charge accumulation on the sample. For some fibers however gold coating was necessary in order to facilitate charge dissipation. The samples were placed on a carbon tape on a circular sample holder and loaded in a vacuum chamber maintained at a pressure of 1.5 x 10^{-5} torr. Fiber diameter measurements were taken, and fiber surfaces and web structure observed and photographed.

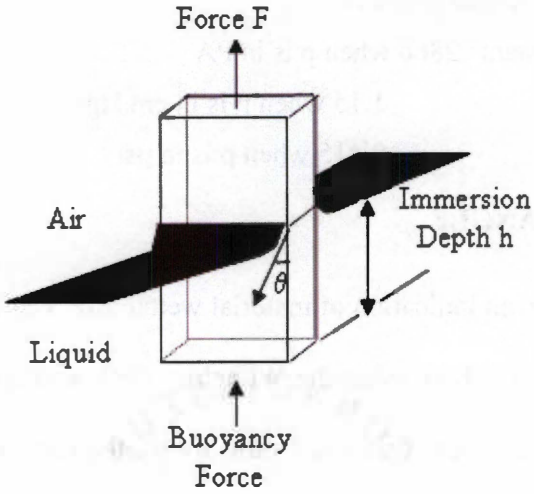

Figure 3.5 Wilhelmy method

3.5.9 X-RAY DIFFRACTION

Determination of degree of crystallinity and orientation in the polymers was carried out using a wide angle x-ray diffraction (WAXD). A 2θ scan was made for one hour and collected on a photo plate which was later scanned and data were exported and processed using software program.

Chapter 4 Results and Discussions

4.1 IL/CELLULOSE RHEOLOGY

The shear rheology of IL/cellulose solution was determined on the ARES instrument at three different temperatures (Figure 4.1 -Figure 4.3). The viscosity for the 7% solution at 100°C appears to be almost constant which is a characteristic of Newtonian behavior, i.e. the viscosity is constant irrespective of the angular velocity. For all other concentrations of the IL/cellulose solutions, at all temperatures, the viscosity decreased with angular velocity, which is termed shear thinning or pseudoelastic behavior for polymer fluids. At most temperatures except for 7% at 100°C the IL/cellulose dope behaved more like a non-Newtonian fluid. The decrease in viscosity with increase in temperature is another characteristic of non-Newtonian fluids which is helpful in the processing of the solution. The IL/cellulose 3, 7 and 10% solutions were found to be more appropriate for electrospinning due to the proximity of their viscosities at 100°C to the viscosities of other polymer fluids that have been electrospun successfully [92].

4.2 THERMAL ANALYSIS

4.2.1 DSC

DSC runs were made on the NMMO/cellulose and IL/cellulose solution in order to study the solution behavior with change in cellulose concentration. As can

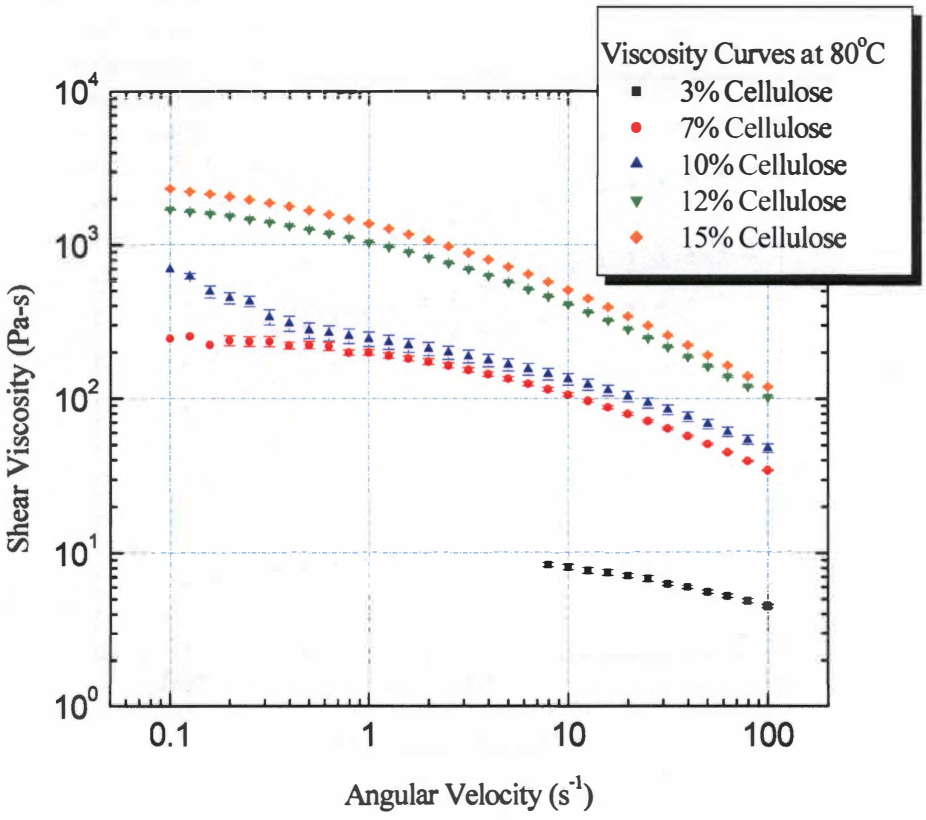

Figure 4.1 IL/cellulose viscosity curves at 80°C

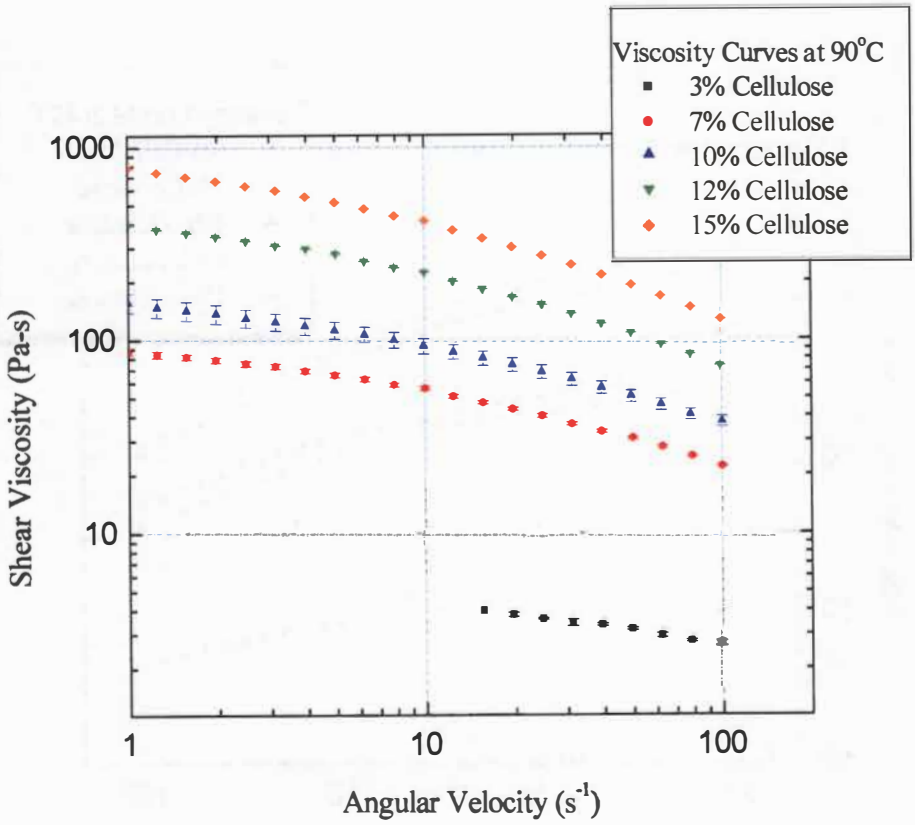

Figure 4.2 IL/cellulose viscosity curves at 90°C

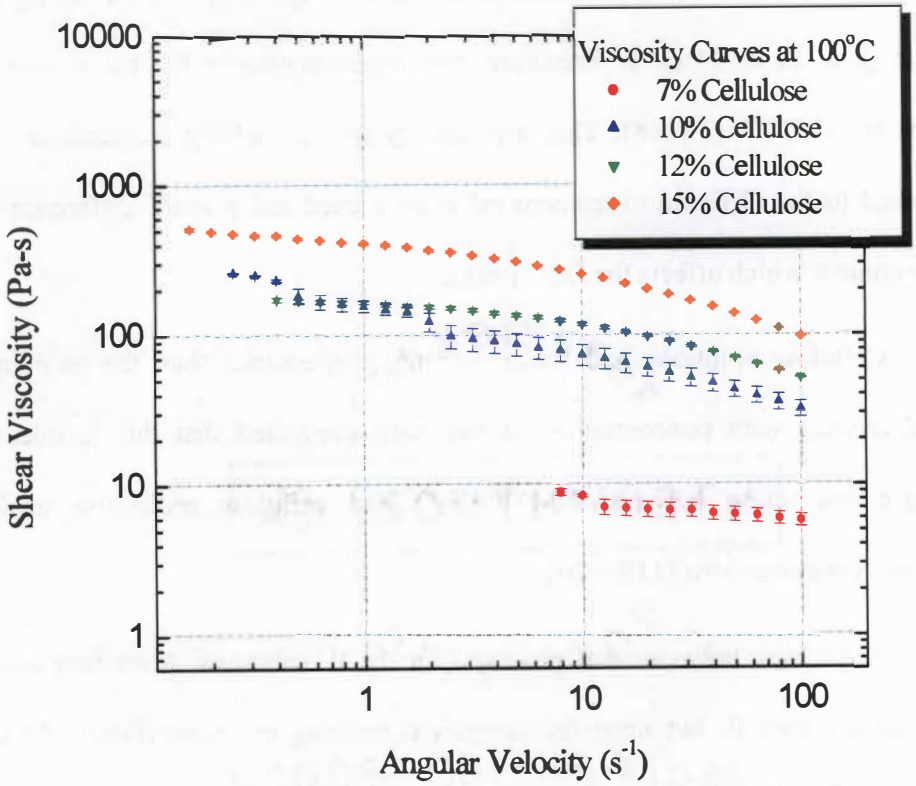

Figure 4.3 IL/cellulose viscosity curves at 100°C

be seen from Figure 4.4 the melting peak shifted to the left at higher cellulose concentration. The melting temperature of NMMO•H_2O was 77.02°C along with a second peak at 80.54°C. In literature, melting temperature for the monohydrate ranges from 72-78°C [118]. This discrepancy in the melting temperature can be attributed to the different instrument calibration used and a small difference in the water content which affects the DSC peaks.

Cellulose solutions had lower melting temperatures than the monohydrate and decreased with concentration. It has been suggested that this is due to the stronger interaction between NMMO•H_2O and cellulose molecules at higher cellulose concentrations [119, 120].

A different behavior was observed for the IL solutions. A melting peak was obtained for pure IL but none for samples containing cellulose (Figure 4.5). This indicated that IL/cellulose solution never recrystallized once the solution was prepared. It was observed visually that the solution was not completely solid at room temperature in the vials. To verify this behavior, DSC trials were repeated with the frozen samples prepared in liquid nitrogen for an hour before testing, again no melting peaks were obtained (Figure 4.6) supporting the theory that there is no recrystallization after the cellulose is dissolved in the IL. Apparently the solution went through a glass transition rather than crystallizing.

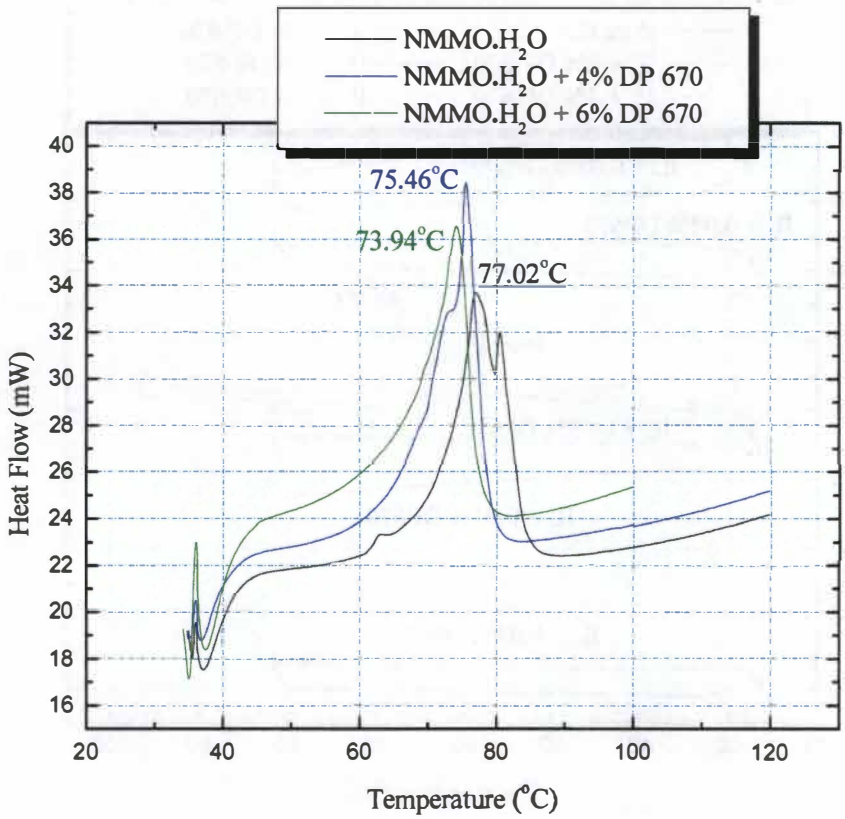

Figure 4.4 DSC graphs for lyocell (NMMO/cellulose)

Hold for 1.0 min at 35.00°C
Heat from 35.00°C to 120.00°C at 10.00°C/min

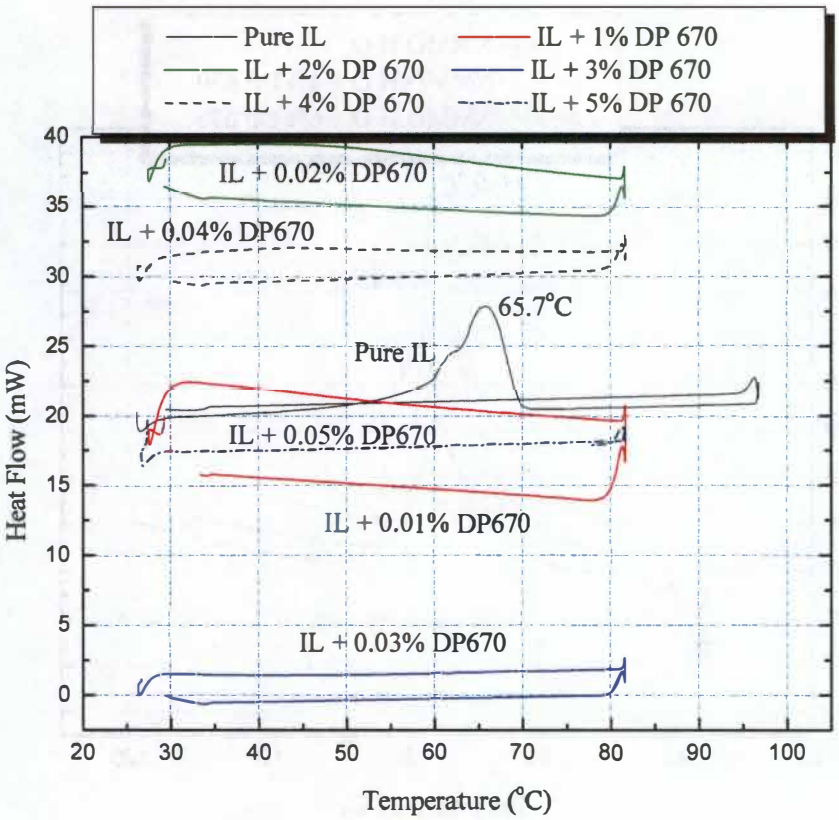

Figure 4.5 DSC graphs for IL/Cellulose

Hold for 1.0 min at 30.00°C
Heat from 30.00°C to 100.00°C at 5.00°C/min
Hold for 1.0 min at 100.00°C
Cool from 100.00°C to 30.00°C at 5.00°C/min

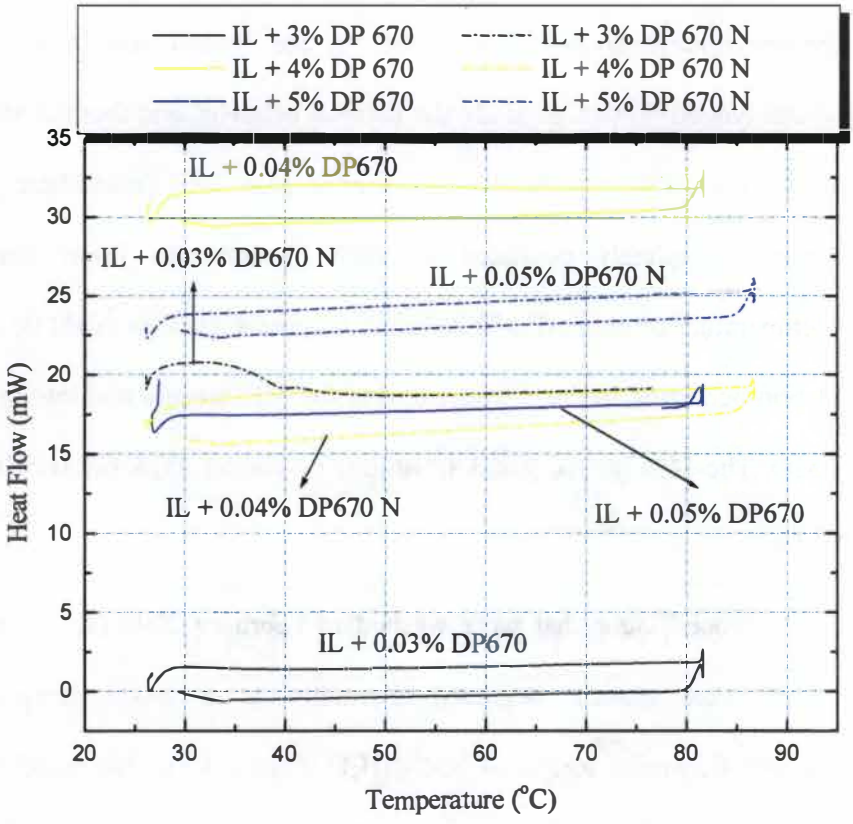

Figure 4.6 DSC Graphs for IL/cellulose frozen in liquid nitrogen

Hold for 1.0 min at 30.00°C
Heat from 30.00°C to 90.00°C at 5.00°C/min
Hold for 1.0 min at 90.00°C
Cool from 90.00°C to 30.00°C at 5.00°C/min

4.2.2 TGA

Thermogravimetric analysis was done on the lyocell solutions, the IL solutions and the lyocell fabrics, to study the thermal behavior and thermal stability of these systems. The 14% webs that were washed in May 2004 (immediately after processing) were completely degraded at 300°C which was lower than the degradation temperature of pure DP 670 cellulose (Figure 4.7). This might be due to some degradation occurring in the extruder during the MB process and due to some residual NMMO. The 14% lyocell solution exhibited a similar TGA behavior to that of NMMO•H_2O.

The 14% lyocell webs that were washed in February 2005 (seven months after the webs were made), degraded thermally at a lower temperature, approximately 200°C, similar to that of NMM•H_2O (Figure 4.8). This could be due to two reasons: cellulose degradation that occurs in the extruder while melt blowing; and/or prolonged exposure of the webs to NMMO which might have lowered the molecular weight of the cellulose (Figure 4.9).

Unlike lyocell, the IL solutions were very similar to the pure IL (Figure 4.10). A comparison was made between lyocell and IL solution to study their thermal degradation behavior and it was found that ILs are more thermally stable than the NMMO monohydrate (Figure 4.11) and can therefore be processed at higher temperature without undergoing thermal degradation.

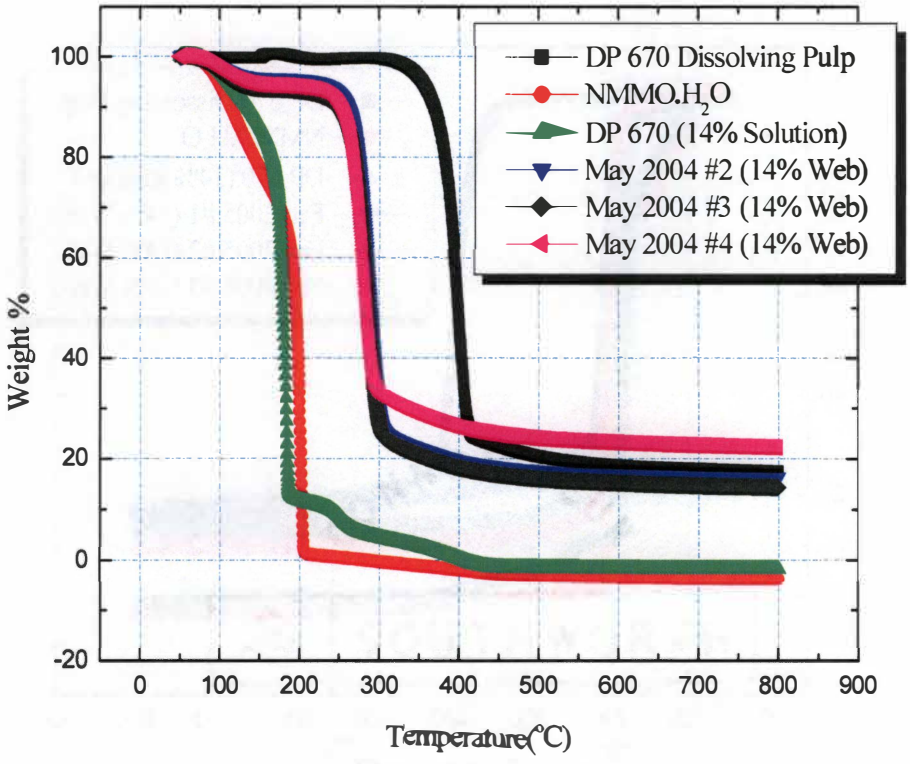

Figure 4.7 TGA for lyocell MB webs washed in May 2004

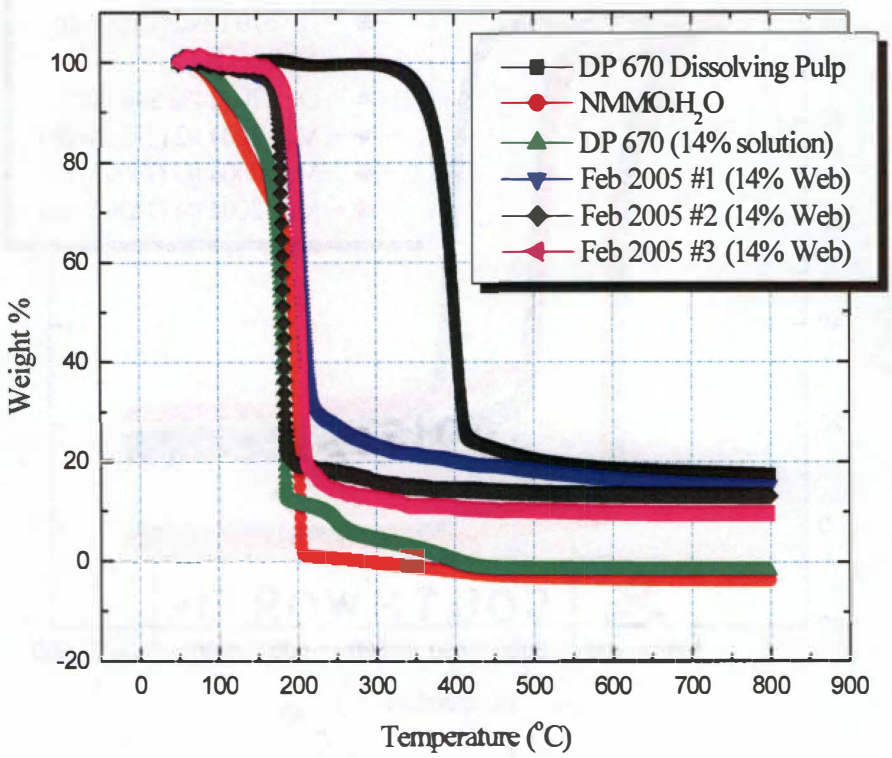

Figure 4.8 TGA for lyocell MB webs washed in February 2005

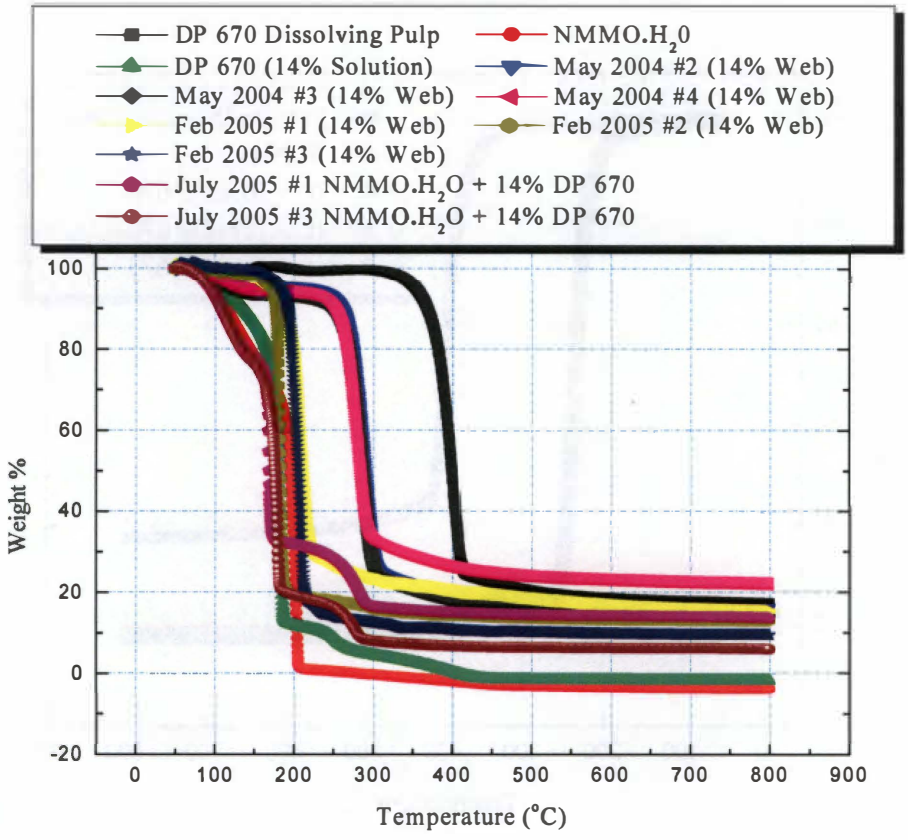

Figure 4.9 TGA for lyocell MB webs

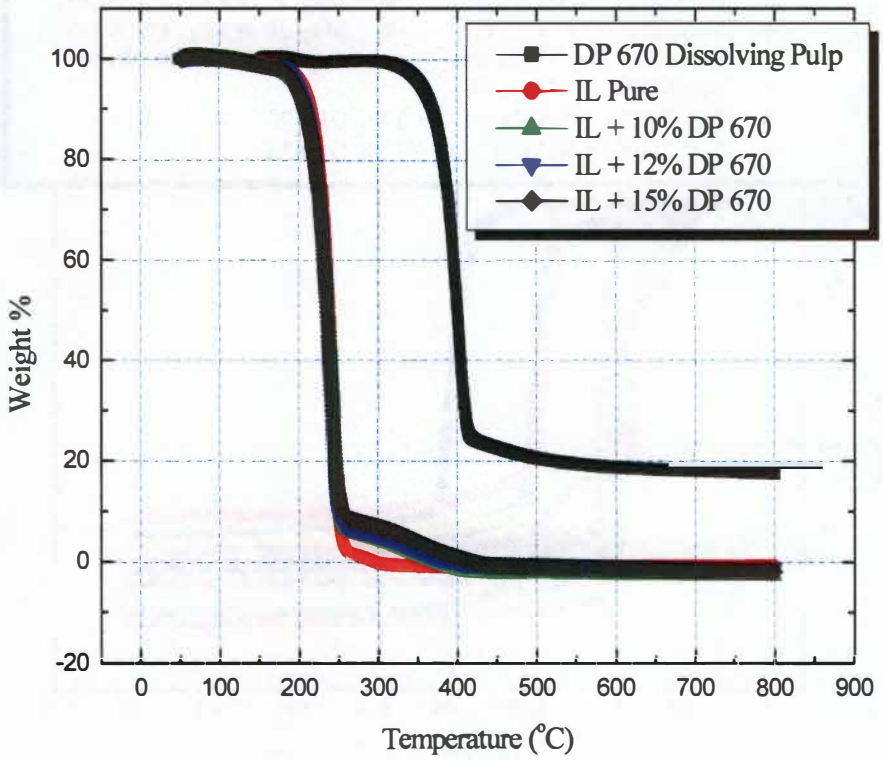

Figure 4.10 TGA for IL/cellulose solution

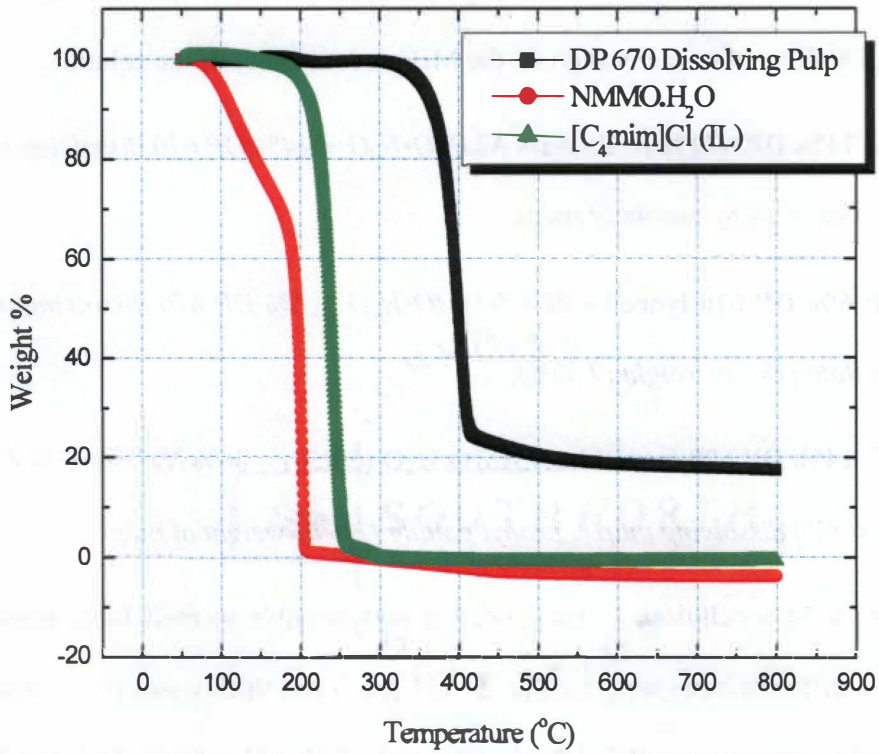

Figure 4.11 TGA for NMMO•H_2O and IL

4.3 LYOCELL MELT BLOWING

Two different concentrations of lyocell (14% and 6%) were selected in order to study the effect of concentration on the MB processability of the solution.

Batch A: 14% DP 670 lyocell - *86% NMMO•H_2O + 14% DP 670 dissolving pulp + propyl gallate (1% by weight of pulp).*

Batch B: 6% DP 670 lyocell - *94% NMMO•H_2O + 6% DP 670 dissolving pulp + propyl gallate (1% by weight of pulp).*

Batch C: 14% DP 670 lyocell in NMMO/H_2O (50/50) – 86% *NMMO/H_2O (50/50) + 14% DP 670 dissolving pulp + propyl gallate (1% by weight of pulp).*

With 14% cellulose in the lyocell it was possible to melt blow nonwoven webs with different basis weights (27, 79, 141 g/m^2) and thicknesses (0.3-0.9 mm) at different die temperatures (97, 100, 113°C) and DCDs (24, 36 in). At lower DCDs spitting was observed and no web was obtained. Increasing the DCD resulted in the production of very thin webs. Since the web collected was very thin it was difficult to remove from the collector, so the collector was allowed to rotate for 15-20 minutes to deposit the several thin layers in a thicker web. Once the web was obtained it was kept in a coagulation bath containing tap water at room temperature for 24 hours and then later was washed several times with deionized water and dried in open air.

The 6% cellulose solution could not be processed into a web because the concentration was too low and spinnability too poor. The solution could be seen dripping from the edge of the die.

Another set of experiments was tried by melt blowing 14 % cellulose mixed with 86% NMMO/H_2O (50/50) so as to shorten the process by avoiding the step of making the NMMO•H_2O separately. It was hypothesized (Figure 4.12) that NMMO•H_2O could be achieved in the twin screw extruder from NMMO/H_2O (50/50) by evaporating the excess water through the vents in the extruder. However this arrangement did not seem to work as the NMMO•H_2O form was apparently not achieved because causing undissolved cellulose to clog the holes in the die.

4.3.1 LYOCELL MB NONWOVEN WEB CHARACTERIZATION

The lyocell nonwoven webs were divided into two different sets. The first set consisted of samples which were washed the day of processing (May 2004) to remove the NMMO. The second set of samples was washed seven months later (February 2005). Both sets of samples were tested for tensile strength, fiber diameter, absorbency, bubble point, and web structure. The fiber diameter varied from 0.8 to 6.23 microns for the webs with an average of approximately 2.3 microns.

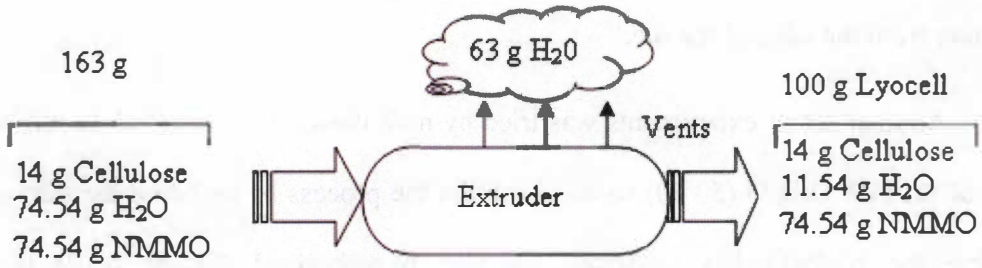

Figure 4.12 Outline diagram NMMO/H_2O (50/50) run

4.3.1.1 TENSILE STRENGTH

The nonwoven MB samples obtained were not large enough to provide standard size specimens for tensile strength measurements. A specimen size of 1 x 3 inch was therefore used. Test results are as shown in Table 4.1.

4.3.1.2 ATS ABSORBENCY

The ATS absorbency results for different basis weights and two different sets of samples are shown in Figure 4.13. The lower basis weight samples that were washed in February 2005 showed higher absorbency compared to the samples washed in May 2004. This might be partly due to a difference in web structure as shown in Figure 4.14 and Figure 4.15, where the fibers were fused with each other resulting in a perforated sheet and there were very few individual fibers. The TGA analysis showed that the degradation temperature of the webs washed in February 2005 was lower than those washed in May 2004. This might be a due to change in molecular structure (DP) of the cellulose due to prolonged exposure to NMMO. The higher basis weight samples were unable to absorb water after the initial 5-6 seconds of the test due to change in sample conformation, whereas the lower basis weight did absorb water for almost 400 seconds. In order to avoid the change in conformation of the thicker samples a non-absorbing hydrophobic fabric was used as the top support and measurements were recorded for first 20 seconds (Figure 4.16). It was observed that with a top support, the thicker samples over flooded within the first

Table 4.1 Test results for lyocell webs

Sample ID	Average. Basis Wt. (g/m^2)	Normalized Peak Force (kg)	Normalized Peak Elongation (%)
May 2004 #2	27.165	MD 2.58 / CD 0.97	MD 104/CD 239
May 2004 #3	141.65	MD 2.9 / CD 3.13	MD 14.5 / CD 14
May 2004 #4	79.5	MD 0.99	MD 12.45

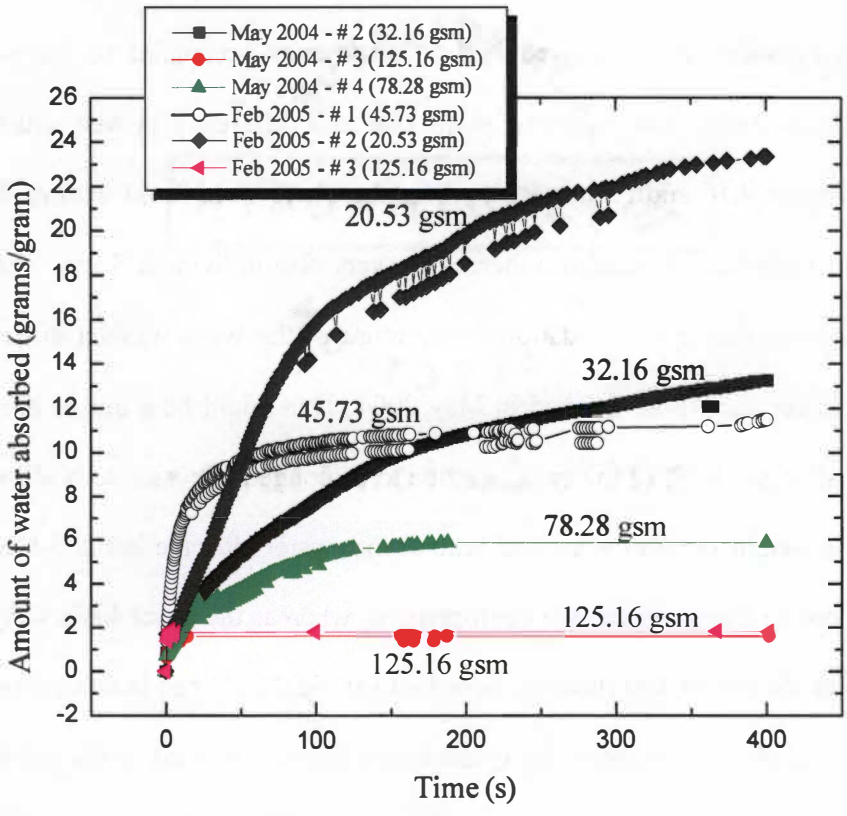

Figure 4.13 ATS absorbency measurements for 400 seconds

(a) Sample 2

(b) Sample 2

(c) Sample 2

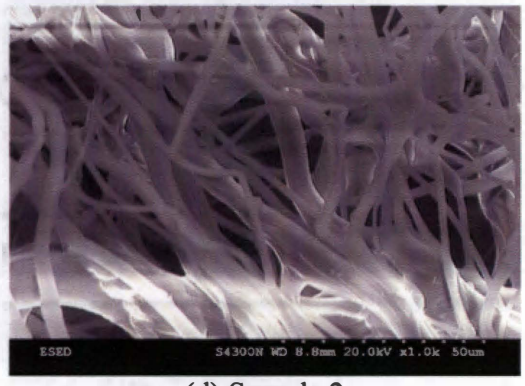

(d) Sample 2

(e) Sample 3

(f) Sample 3

Figure 4.14 SEM micrographs of 14% lyocell MB nonwoven webs washed in May 2004

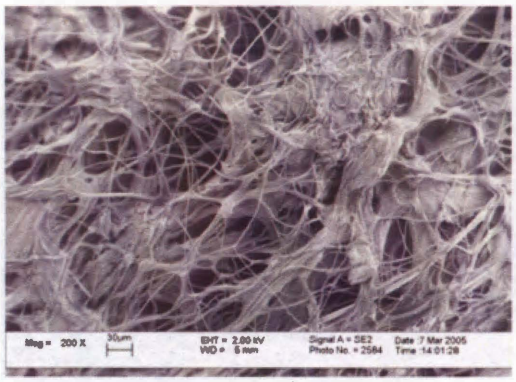

(a)Sample 1

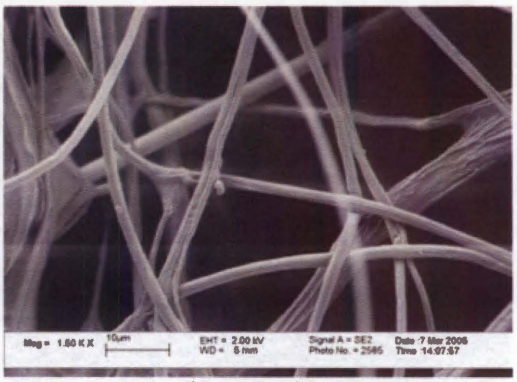

(b) Sample 1

(c)Sample1

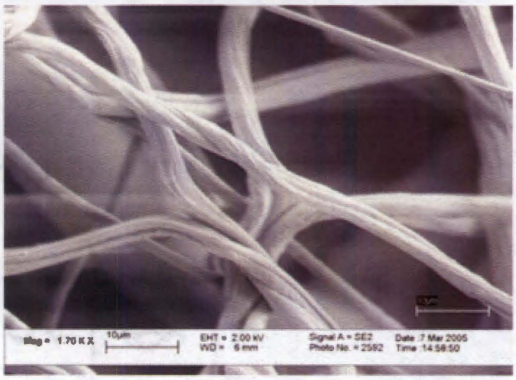

(d) Sample 2

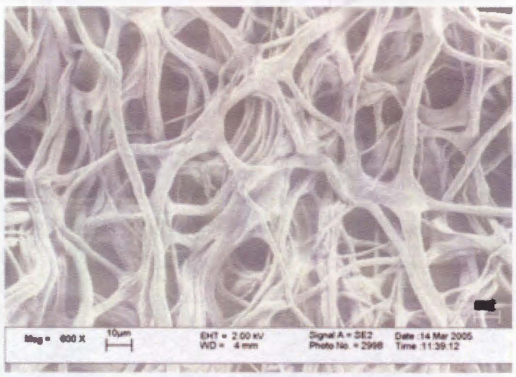

(e) Sample 3

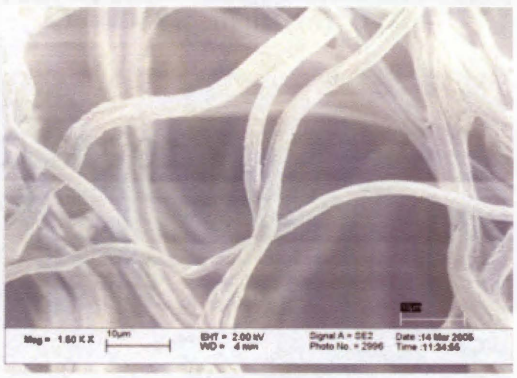

(f)Sample3

Figure 4.15 SEM micrographs of 14% lyocell MB nonwoven webs washed in February 2005

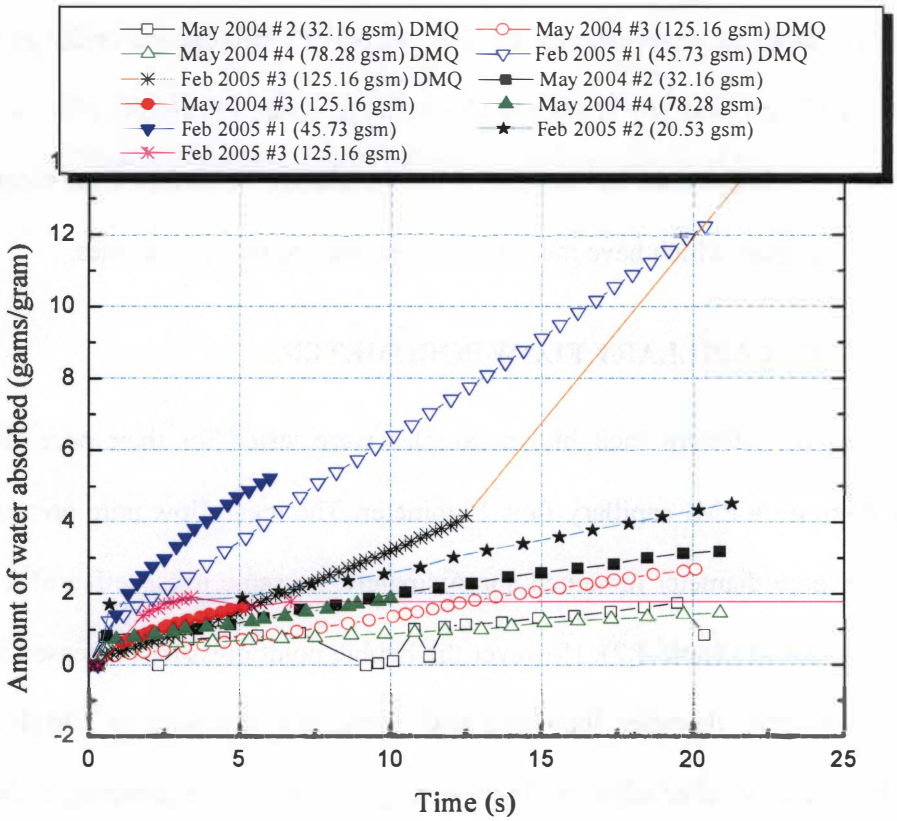

Figure 4.16 ATS absorbency measurements for first 20 seconds

17-18 seconds and measurements could not be made on all the samples. However, this did show that thicker samples absorbed at a higher rate than thinner samples.

The samples were examined under an optical microscope under polarized light to see if there was any change in shape due to water absorption. Fiber swelling was observed which could be one reason for the change in surface conformation of the thicker samples which have more fibers compared to thinner samples.

4.3.1.3 PMI CAPILLARY FLOW POROMETER

The six different melt blown samples were tested for their pore size and bubble point on a PMI capillary flow Porometer. The mean flow pore pressure and mean flow pore diameter remained approximately the same irrespective of the time they were washed (Table 4.2). However the bubble point pressure decreased and the bubble point pore diameter increased with prolonged exposure to NMMO. This might be due to smaller adjacent fibers fusing together in the presence of NMMO thereby resulting in bigger pores and was confirmed by SEM micrographs (Figure 4.14, Figure 4.15, Figure 4.17) where it was more difficult to locate single fibers in samples that were washed later compared to those that were washed the same day of manufacturing. Several micrographs were taken with different magnification in order to better observe the web structure. Also the fusing of fibers in the presence of NMMO was indicated by the broader pore size distribution for the MB samples that were washed in February 2005. It was observed that samples washed in May 2004

Table 4.2 PMI measurements

Sample ID	May2004 # 2	May2004 # 3	May2004 # 4	Feb 2005 # 1	Feb 2005 # 2	Feb 2005 # 3
Mean Flow Pore Pressure (KPa)	2.48	2.48	1.72	1.9	2.07	2.21
Mean Flow Pore Diameter (μm)	17.78	18.13	26.21	22.45	21.52	20.56
Bubble Point Pressure (KPa)	1.1	0.076	0.007	0.007	0.007	0.007
Bubble Point Pore Diameter (μm)	39.66	578.0	7986	6165	7191	9112

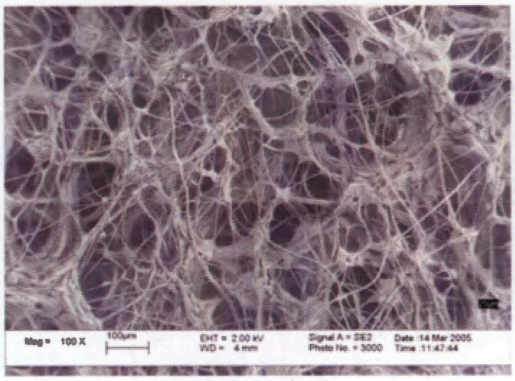

(a)Sample 1

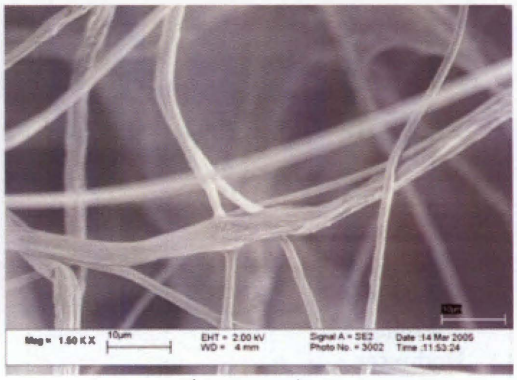

(b) Sample 1

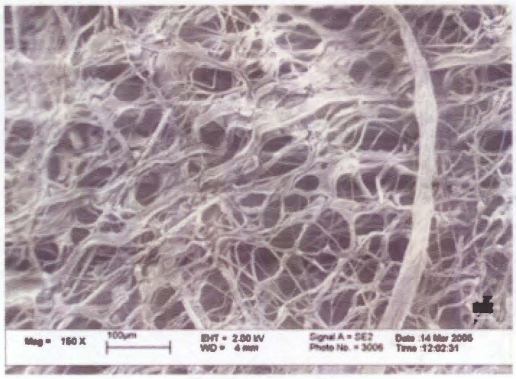

(c)Sample2

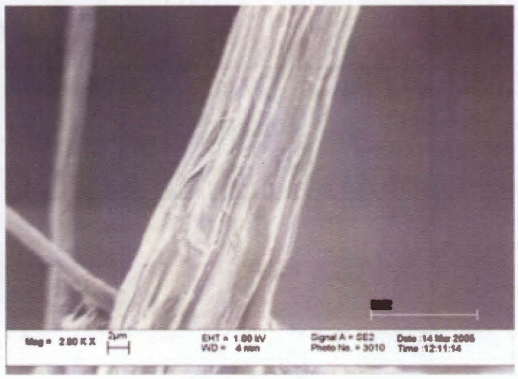

(d) Sample 2

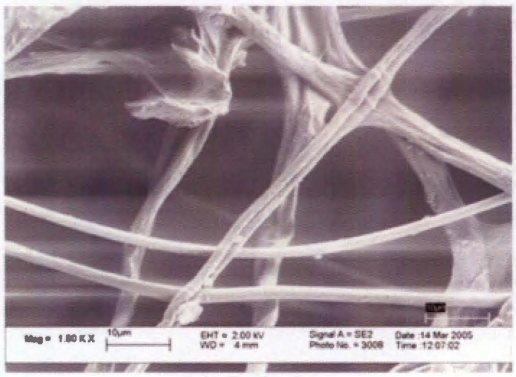

(e) Sample 2

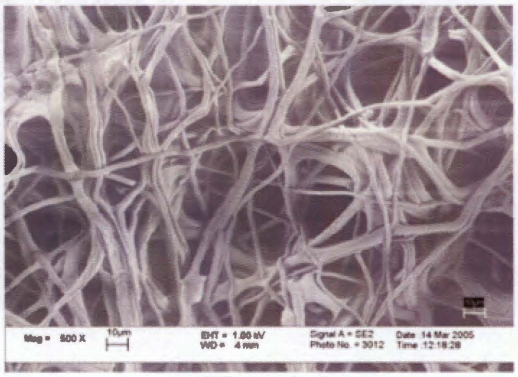

(f)Sample3

Figure 4.17 SEM micrographs unwashed 14% lyocell MB nonwoven webs

had a narrower distribution compared to samples washed in February, which can again be attributed to the fusion of fibers leading to bigger pore diameter and wider distribution.

4.3.1.4 CONTACT ANGLE

The difference between the advancing and receding contact angle was lower for samples washed in February 2005 indicating a more wettable surface (Table 4.3).

4.4 IL/CELLULOSE ELECTROSPINNING

The first set of experiments was conducted in the normal configuration of grounding the metal collector and charging the needle with processing conditions given in Table 4.4. For the 3% cellulose solution at low voltage, there was no bubble formed at the end of the needle. The voltage was increased to induce solution extrusion, but above 18 KV, there was charge leakage and arcing. The polarity was then reversed by charging the collector and grounding the needle, allowing higher voltages up to 40 KV to be reached. This resulted in production of fine fiber streams from the needle, but the fibers fused upon contacting the collector. Apparently the fibers did not coagulate when exiting the die and, with this high concentration of solvent, fused at the collector surface. The experiment did however confirm that the electrospinning technique could be used for the IL/cellulose solutions. A further trial with the 7% solution did not result in fiber formation because the higher

Table 4.3 Contact angle measurements

Sample ID	Advancing Angle	Receding	Hysteresis
May 2004 # 2	55.3	25.1	30.2
May 2004 # 3	50.7	21.7	29.0
May 2004 # 4	47.3	24.3	23.0
Feb 2005 # 1	40.5	34.7	5.8
Feb 2005 # 2	37.4	30.5	6.9
Feb 2005 # 3	47.6	31.0	16.6

Table 4.4 Processing conditions for IL electrospinning

Solution Concentration	Syringe temperature (°C)	Needle Diameter (mm)	Throughput (ml/min)	Voltage Applied (KV)	Needle to collector distance (cm)
IL+3% Cellulose	95	0.41	0.0114-0.1026	28-30 KV	7.62
IL+7% Cellulose	100	0.91	0.0912–0.1026	28-30 KV	7.62

concentration solution was too viscous for the initial apparatus and spinning condition.

In a second series of experiments, two changes were made to enable the 7% solutions to be processed. First the diameter of the syringe needle was increased from 0.41 to 0.91 mm. Secondly, the temperature of the solution and syringe was increased from 95 to 100°C. In addition the needle was heated intermittently during the run to maintain the temperature and hence the viscosity of the solution. This setup gave good fibers but the forces resulting in fiber formation differed from those normally associated with electrospinning. The separation of fine fibers in the electric field was not apparent, but rather a large fiber stream exited the needle and then exhibited a flapping or vibrating motion which resulted in individual fibers. The flapping jet seemed consistent in shape and size. The minimum distance between needle and the collector that could be achieved without arcing was 76.2 mm.

4.4.1 IL/CELLULOSE ELECTROSPUN WEB CHARACTERIZATION

The webs obtained with the 7% solution and modified apparatus were examined under the SEM (Figure 4.18). The fibers obtained were larger than expected for electrospinning mainly because of the nonevaporating solvent which assists in fiber diameter reduction and orientation. As the fibers touch the collector they are still wet and formable resulting in shapes from circular to flat (Figure 4.18a). However the fibers that did not contact the collector and got laid over other fibers retained the circular shape Figure 4.18(d). The fiber diameters ranged from

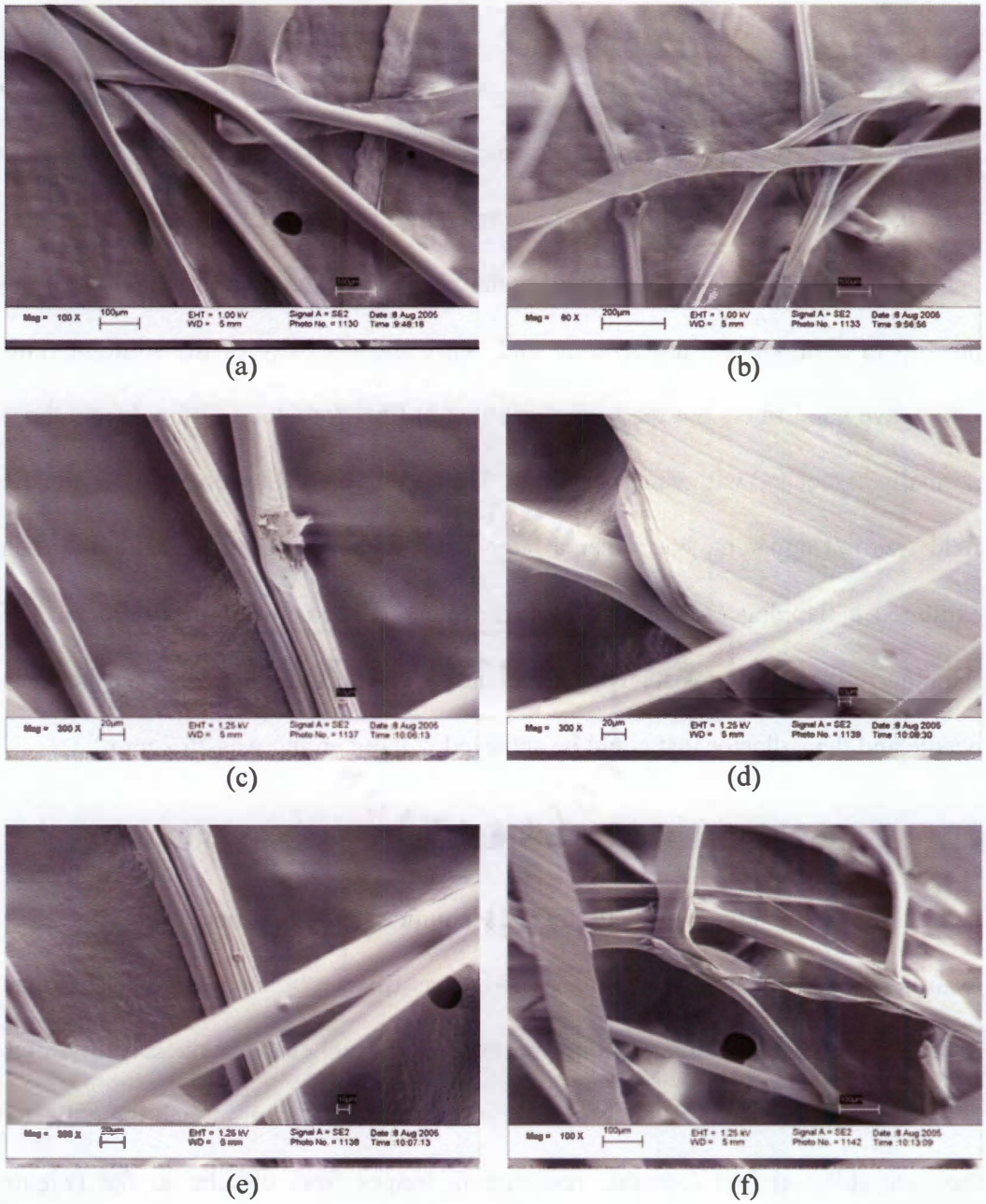

Figure 4.18 SEM micrographs of IL/Cellulose electrospun nonwoven webs

17 – 25 microns. Also the fiber surface was smooth (Figure 4.18) unlike lyocell fibers and was brittle which might again be due to low orientation.

4.5 IL/CELLULOSE ACER ASSITED SPINNING

Four sets of trials were made with different processing conditions as shown in Table 4.5. It was possible to spin fibers from the 12% solution under the processing conditions selected. For the 15% concentration however the extruded fibers broke easily and could not be drawn. A problem in all the spinning runs was the bubbles in solution which lead to discontinuous spinning. Several techniques were tried to get rid of the bubbles: holding the sample in a vacuum over for 3 hours at 100°C and placing it the barrel for one hour at the set temperature before spinning. Neither was effective in reducing the bubbles.

The fibers were tested for strength and diameter and the surface was observed microscopically. The tensile properties are given in Table 4.6. Single fiber properties were found to be superior in terms of higher elongation and tenacity when compared to the existing cellulose fibers in the market (Table 2.2). When strength of the fiber bundles was measured however only half broke, therefore generating false values (Table 4.6).

The fibers were spun in a range of 12.7 – 84.5 microns diameter. They were very smooth and silk like, free from any surface irregularities (Figure 4.19) unlike the lyocell fibers and had a superior hand which is an advantage to

Table 4.5 Processing condition for ACER assisted spinning

Sample ID	Solution Conc.	Barrel Temperature (°C)	Ram Speed (sec^{-1})	Winding Speed (m/min)	Distance Between Die and Bath (cm)
T105-1.0	12%	105	1.0	100	16.51
T100-2.0	12%	100	2.0	100	16.51
T100-2.5	12%	100	2.5	100	16.51
T115-3.0	15%	100-115	1-3.0	100	16.51

Table 4.6 Fiber bundle strength

Sample ID	Fiber Diameter (μm)	Maximum Load (kgf)	Maximum Elongation (%)	Tenacity (g/den)
T105-1.0 (Single fiber)	24	0.035	37.17	5.65
T105-1.0 (Bundle strength)	24	0.658	13.564	2.08
T100-2.0 (Bundle strength)	34	0.903	13.425	1.37
T100-2.5 (Bundle strength)	38	1.021	10.98	1.32

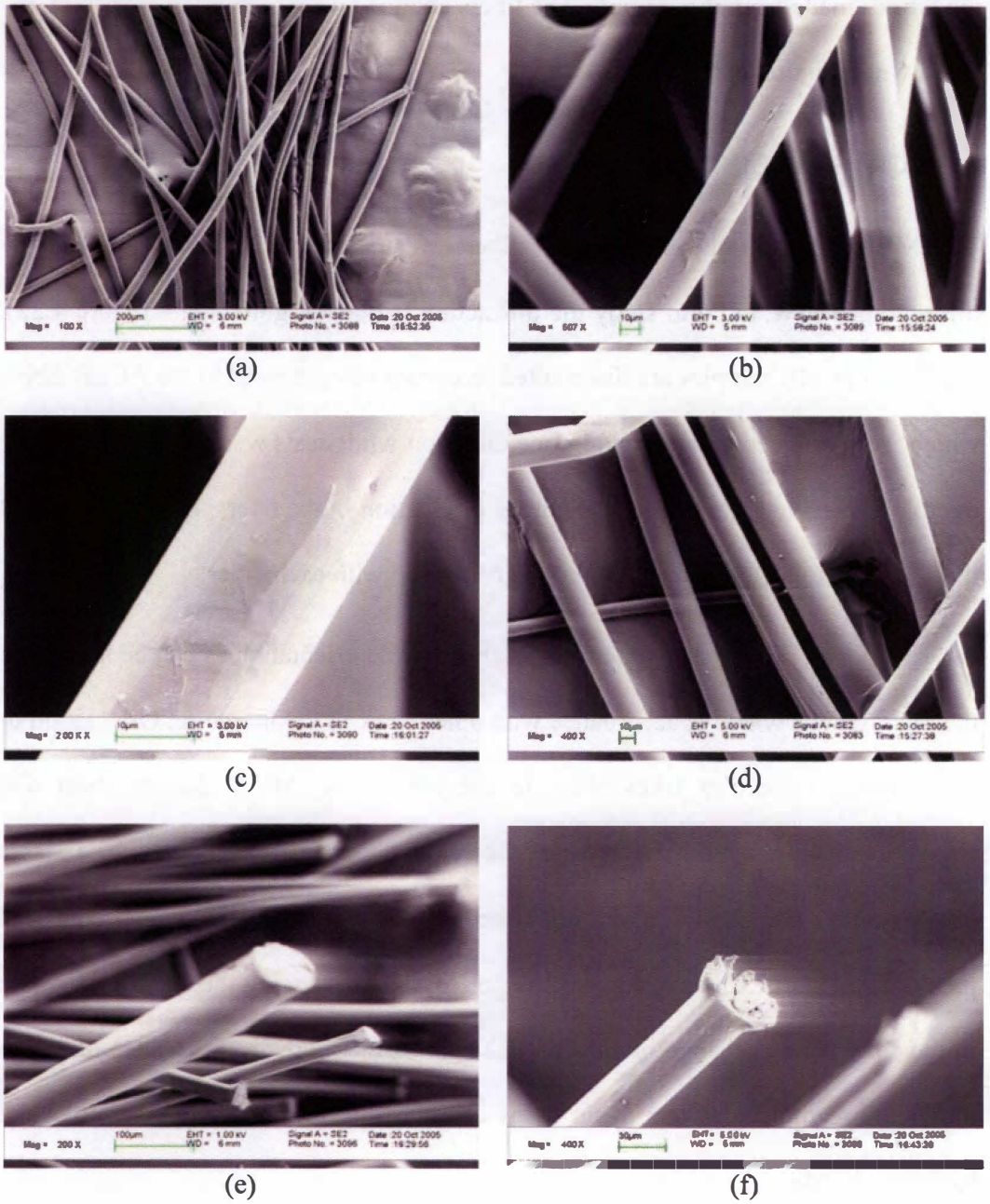

Figure 4.19 SEM micrographs of IL/Cellulose fibers

the fabrics made from these fibers. The fibers obtained were circular in cross section as shown in Figure 4.19 - Figure 4.20.

4.6 CRYSTALLINITY

The MB webs and the single spun fibers were tested on a wide angle x-ray diffractometer (WAXD) to study the diffraction pattern (Figure 4.21 - Figure 4.22). The fibers in MB samples are disoriented so cannot be compared to the ACER fibers which were oriented and aligned in one direction while tests were performed. These micrographs gave a general idea about the orientation in the fibers; however since all the samples are different these cannot be compared with each other.

The ACER assisted spun fibers showed some orientation as can be seen from the micrographs which is accordance with other work in the literature. Orientation of the polymer molecules takes place in the die of the ACER due to shear and elongational deformation. Because of the relatively long relaxation time, a stable orientational state is preserved until the extrudate gets to the water bath and precipitation starts. The air gap plays major role in influencing the chain orientation in the fiber. The exchange of solvent (IL) against the non-solvent (water) dissolves the cellulose molecules and again helps in reforming the intra and intermolecular hydrogen bonds.

Figure 4.20 Cross section of the fibers obtained by microtoming the samples and using leica confocal laser microscope

DP 670 Cellulose sheet

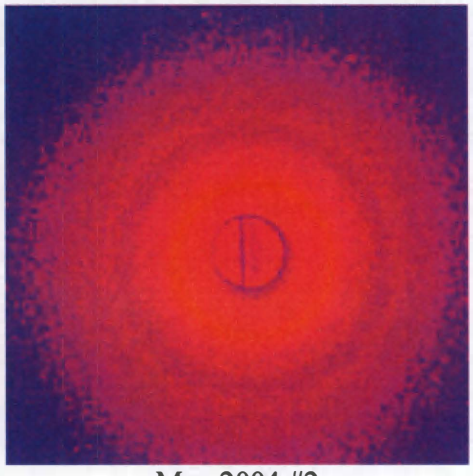

May 2004 #2

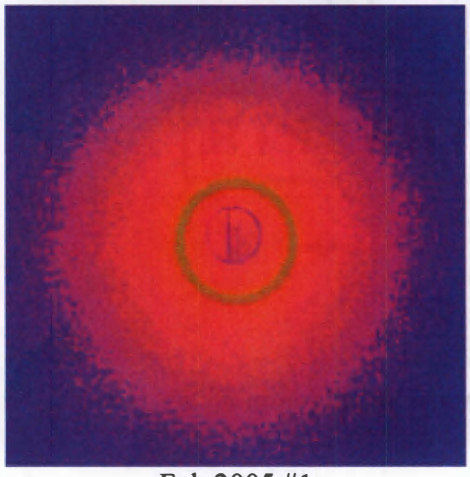

Feb 2005 #1

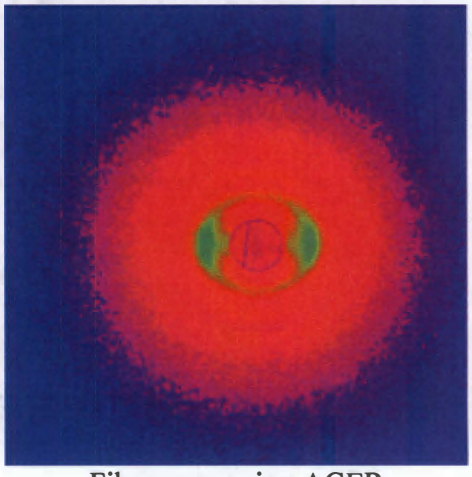

Fiber spun using ACER

Figure 4.21 X-Ray Micrographs

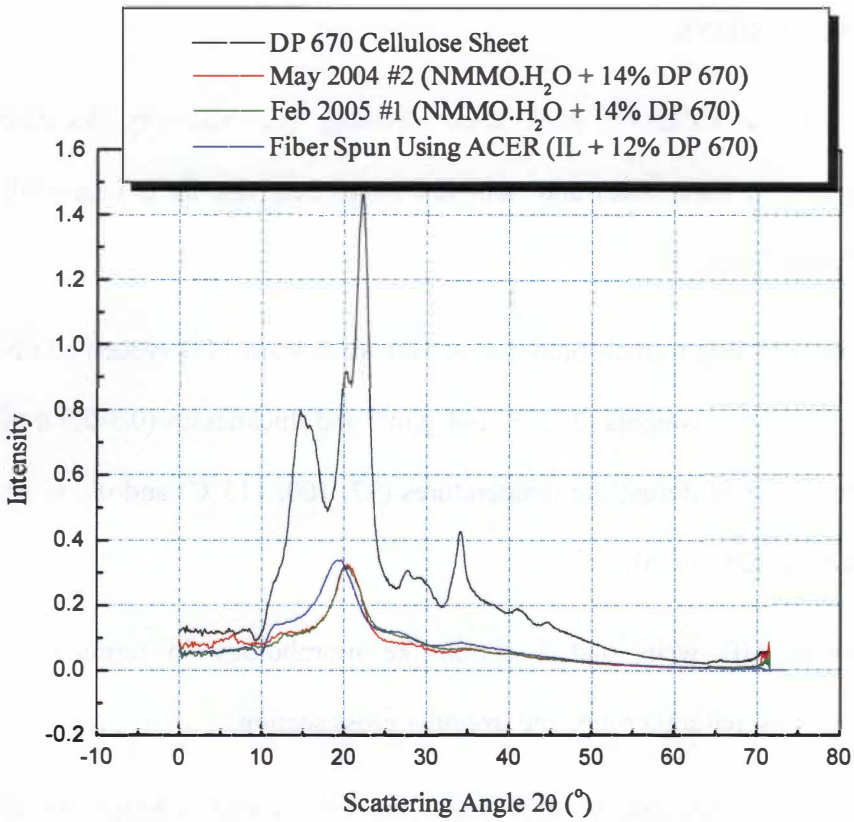

Figure 4.22 Intensity Vs scattering

Chapter 5 Conclusions and Future Work

5.1 CONCLUSIONS

- IL/cellulose solutions show shear thinning (i.e. viscosity decrease with increase in shear rate) and non-Newtonian behavior as is case with other polymer fluids.
- It was possible to melt blow nonwoven webs from 14% lyocell solutions. A range of basis weights (27, 79, 141 g/m^2) and thicknesses (0.3-0.9 mm) were produced at different die temperatures (97, 100, 113°C) and die to collector distances (24, 36 in).
- Lyocell MB webs had a cotton-like morphology in terms of surface roughness, natural crimp, and irregular cross section.
- It was not possible to melt blow the 6% lyocell solution because the concentration was too low and the spinnability too poor.
- Prolonged exposure to NMMO leads to degradation of the cellulose at the molecular level.
- IL solutions are thermally more stable than NMMO and can be processed at higher temperatures without undergoing degradation.
- IL/cellulose solutions do not recrystallize after the solution is prepared.
- Lyocell webs have good water absorbency.

- It was possible to electrospin IL/cellulose fibers; however the fiber diameter was bigger than the expected diameter for electrospun fibers. Water should be used in the system to regenerate the cellulose.
- IL/cellulose solutions are spinnable and the regenerated ACER spun fibers have better tenacity and elongation than the current manufactured cellulosic fibers. The fibers obtained were smooth and silk like.
- There is a potential to increase the fiber properties i.e. tenacity and elongation by making a more homogenous bubble-free IL solution and increasing the winding speed.

5.2 FUTURE WORK

- A water jet spray should be added to the MB apparatus to facilitate the cellulose precipitation instead of doing it later.
- The electrospinning of IL/cellulose should be carried out in a grounded water bath and 3% solutions should be used since they gave better cone formation and fiber jets.
- For ACER assisted spinning a better feeding system is required which would get rid of the bubbles in the systems that are responsible for breaking of the spin line during the process.
- Spinning of IL/cellulose can be tried at higher temperatures (115°C for 15%) since ILs are stable up to 200°C and do not explode unlike NMMO.

References

References

1. Lin, C. W., Hazardous Air Pollutant Source Emissions from Fiber Manufacturing Facility in Taiwan, *Water, Air and Soil Pollution*, **128**, 321, 2001.

2. Wolschner, B., Weber, H., Linde, V. F., Peritsch, M., Cellulosic Fiber Industry - Economic and Ecological Aspects of Further Developments, *Chemical Fibers International*, **45**(1), 41, 1995.

3. Mukherjee, S., Biswas, M. N., Roy, N. C., Abatement of Air Pollution in Rayon Plants - A Review, *Chemical Engineering World*, **24**(12), 27, 1989.

4. http://www.lenzing.com/nonwovens/en/index.jsp

5. Gannon, J. M., Graveson, I., Mortimer, S. A., Process for the Manufacture of Lyocell Fiber, US Patent No. 5,725,821, March 10, 1998, Assigned to Courtaulds Fibres (Holdings) Limited.

6. Luo, M., Roscelli, V. A., Neogi, A. N., Sealey, J. E., Jewell, R. A., Lyocell Fibers, and Compositions for Making the Same, US Patent No. US 6,210,801 B1, April 3, 2001, Assigned to Weyerhaeuser Company.

7. Luo, M., Roscelli, V. A., Camarena, S., Neogi, A. N., Yancey, M. J., Gaddis, P. G., Process for Melt Blowing Continuous Lyocell Fibers, US Patent No. US 6,306,334 B1, October 23, 2001, Assigned to Weyerhaeuser Company.

8. Luo, M., Roscelli, V. A., Neogi, A. N., Jewell, R. A., Lyocell Nonwoven Fabric and Process for Making, US Patent No. 6,596,033 B1, July 22, 2003, Assigned to Weyerhaeuser Company.

9. Klemm, D., Heublein, B., Fink, H. P., Bohn, A., Cellulose: Fascinating Biopolymer and Sustainable Raw Material, *Angewandte Chemie, International Edition*, **44**(22), 3358, 2005.

10. Klemm, D., Schmauder, H. P., Heinze, T., *Biopolymers*, **6**, 290, 2002.

11. Kaplan, D. L., Biopolymers from Renewable Resources, Springer, Berlin, 1, 1998.

12. Kim, C. H., Frey, M. W., Marquez, M., Joo, Y. L., Preparation of Submicron-Scale, Electron Cellulose Fibers via Direct Spinning, *Journal of Polymer Science, Part B, Polymer Physics*, **43**, 1673, 2005.

13. Cucolo, J. A., Aminuddin, N., Frey, M. W., Structure Formation in Polymeric Fibers, Salem, D. R., Ef., Hanser Gardner Publications, Inc., Munich, Chap 8, 296, 2001.

14. Krassig, H. A., Cellulose Structure, Accessibility, and Reactivity, Gordon and Breach, Amsterdam, 1993.

15. Rydholm, S. A., Pulping Process, Interscience Publishers, Division of John Wiley & Sons, Inc., 1976.

16. Eichhorn, S. J., Baillie, C. A., Zafeiropoulos, N., Mwaiambo, L. Y., Ansell, M. P., Dufresne, A, Entwistle, K. M., Herrera, P. J., Escamilla, G. C.; Groom, L., Hughes, M., Hill, C.; Rials, T. G., Wild, P. M., Review Current International Research into Cellulosic Fibers and Composites, *Journal of Material Science*, **36**, 2107, 2001.

17. Buschle, G. D.; Fanter C.; Loth, F., Structural Changes in Hemp Fibers as a Result of Enzymic Hydrolysis with Mixed Enzyme Systems, *Textile Research Journal*, **69**(4), 244, 1999.

18. Payen, A., Comptes Rendus Hebdomadaires des Seances de l Academie des Sciences, **7**, 1052. 1938.

19. Zimmermann, R. L., US Patent No. 5,216,154, Assigned to Texaco Chemical Company.

20. O'Sullivan, A., Cellulose: The Structure Slowly Unravels, *Cellulose*, **4**, 173, 1997.

21. Woodcock, C., Sarko, A, Packing Analysis of Carbohydrates and Polysaccharides. 11. Molecular and Crystal Structure of Native Ramie Cellulose, *Macromolecules*, **13**(5), 1183, 1980.

22. Sarko, A, Muggli, R., *ibid*, **7**, 480, 1974.

23. Heuseer, E., The Chemistry of Cellulose, London, John Wiley & Sons, 144.

24. Nevell, T. P., Zeronian, S. H., Cellulose Chemistry, and its Application, New York, Ellis Horwood Ltd., 1985.

25. Glasser, W. G., Pulp and Paper Chemistry and Chemical Technology, Wiley Interscience, New York, 39, 1980.

26. Sjostrom, E, Wood Chemistry Fundamentals and Application, New York Academic Press, 49, 1981.

27. Philipp, B., *Journal of Macromolecular Science, Pure and Applied Chemistry*, **A30**, 703, 1993.

28. Roesnau, T, Potthast, A, Sixta, H., Kosma, P., The Chemistry of Side Reaction and Byproduct Formation in the System NMMO/Cellulose (Lyocell Process), *Progress in Polymer Science*. **26(9)**, 1763, 2001.

29. Adorjan, I., Sjöberg, J, Rosenau, T, Hofinger, A., Kosma, P., Kinetic and Chemical Studies on the Isomerization of Monosaccharides in N-methylmorpholine-N-oxide (NMMO) Under Lyocell Conditions, *Carbohydrate Research*, **339**, 1899, 2004.

30. Rosenau, T, Hofinger, A., Potthast, A., Kosma, P., On the Conformation of the Cellulose Solvent N-Methylmorpholine-N-oxide (NMMO) in Solution, *Polymer*, **44**, 6153, 2003.

31. Lim, K. Y., Yoon, K. J., Kim, B. C., Highly Absorbable Lyocell Fiber Spun from Cellulose/Hydrolyzed Starch-g-PAN Solution in NMMO Monohydrate, *European Polymer Journal*, **39**, 2115, 2003.

32. Kim, D. B., Jo, S. M., Lee, W. S., Pak, J. J., Physical Agglomeration Behavior in Preparation of Cellulose-N-Methyl Morpholine N-oxide Hydrate Solutions by Simple Mixing, *Journal of Applied Polymer Science*, **93**, 1687, 2004.

33. Frank, N. E., Varga, J. K., US Patent No. 4,145,532, Assigned to Akzona Inc.

34. Fink, H. P., Weigel, P., Purz, H. J., Ganster, J., Structure of Regenerated Cellulose Materials from NMMO Solutions, *Progress in Polymer Science*, **26**, 1473, 2001.

35. Meister, G., Wechsler, M., Biodegradation of N-methylmorpholine-N-Oxide, *Biodegradation*, **9**, 91, 1998.

36. Chae, D. W., Kim, B. C., Lee, W. S., Rheological Characterization of Cellulose Solutions in N-Methyl Morpholine N-Oxide Monohydrate, *Journal of Applied Polymer Science*, **86**, 216, 2002.

37. Petrovan, S., Negulescu, I., Collier, J., Elongational and Shear Rheology of Cellulosic and Lignocellulosic Solutions in N-

Methylmorpholine Oxide Monohydrate, *Cellulose Chemistry and Technology*, **35**, 89, 2001.

38. Rosenau, T., Potthast, A., Adorjan, I., Hofinger, A., Sixta, H., Firgo, Kosma, P., Cellulose Solutions in N-Methylmorpholine-N-Oxide (NMMO)-Degradation Process and Stabilizers, *Cellulose*, **9**, 283, 2002.

39. Rosenau, T, Potthast, A, Milacher, W., Hofinger, A., Kosma, P., Isolation and Identification of Residual Chromophores in Cellulosic Materials, *Polymer*, **45**, 6437, 2004.

40. Collier, J. R., Romanoschi, O., Petrovan, S., Elongational Rheology of Polymer Melts and Solutions, *Journal of Applied Polymer Sciences*, **69**, 2357, 1998.

41. Petrovan, S., Collier, J. R., Morton, G. H., Rheolgy of Cellulosic N-Methylmorpholine Oxide Monohydrate Solutions, *Journal of Applied Polymer Science*, **77**, 1369, 2000.

42. Petrovan, S., Collier, J. R., Negulescu, I. I., Rheology of Cellulosic N-Methylmorpholine Oxide Monohydrate Solutions of Different Degrees of Polymerization, *Journal of Applied Polymer Sciences*, **79**, 396, 2001.

43. Collier, B. J., Dever, M., Petrovan, S., Collier, J. R., Li, Z., Wei, X., Rheology of Lyocell Solutions from Different Cellulose Sources, Journal of Polymers and the Environment, **8**(3), 151, 2002

44. Li, Z., Rheology of Lyocell Solutions from Different Cellulosic Sources and Development of Regenerated Cellulosic Microfibers, Dissertation, University of Tennessee, Knoxville, August, 2003.

45. Luo, M., Roscelli, V., Neogi, A., Selby, J., Sealey, J., Camarenan, S., Meltblown and Spunbonded Cellulosic Nonwovens, Processdings of 11th Annual International TANDEC Nonwovens Conference, Nov 6-8, Knoxville, TN, USA.

46. Nevell, T. P., Cellulose Chemistry and its Application, John Wiley and Sons, 1985.

47. Mccorsley, C. C., US Patent No. 4,246, 221, 1981.

48. Coulsey, H., Smith, S., 34th International Man-Made Fibers Congress, 1995.

49. Mortimer, S. A., Peguy, A. A., The Influence of Air Gap Conditions on the Structure Formation of Lyocell Fibers, *Journal of Applied Polymer Science*, **60**, 1747, 1996.

50. Chanzy, H., Paillet, M., Spinning of Cellulose from N-Methylmorpholine N-Oxide in the Presence of Additives, *Polymer*, **31**, 400, 1990.

51. Woodings, C. R., The Development of Advanced Cellulosic Fibers, *International Journal of Biological Macromolecules*, **17**(6), 1995.

52. Doherty, S, Guillard, C., Pichat, P., Kinetics and Products of the Photocatalytic Degradation of the Morpholine (Tetrahydro-2H-1, 4-oxazine) in TiO2 Aqueous Suspensions, *Journal of the Chemical Society Faraday Transactions*, **91**, 1853, 1995.

53. Stockinger, H., Kut, O. E., Heinzle, E., Ozonation of Wastewater Containing N-methylmorpholine-N-oxide, *Water Research*, **30**, 1745, 1996.

54. Gupta, R. K., Polymer and Composite Rheology, Plastics Engineering, Marcel Dekker, Inc.

55. ARES-LS, Instrumental Manual, 902-30026 Rev X1, Preliminary, May 2000.

56. ACER 2000, User manual, 902-40012 Rev A, January 1999.

57. Collier, J. R., Romanoschi, O., Petrovan, S, Elongational Rheology of Polymer Melts and Solutions, *Journal of Applied Polymer Science*, **69**, 2357, 1998

58. Collier, B. J., Dever, M., Petrovan, S., Collier, J. R., Li, Z., Wei, Z., Rheology of Lyocell Solutions from Different Cellulose Sources, *Journal of Polymers and the Environment*, **8**(3), 151, 2000.

59. J. R. Collier, S. Petrovan, B. J. Collier, M. Dever, X. Wei, Z. Li, A. Dahiya, Rheology of Lyocell Solutions from Commercial and Agricultural Residue Sources' (Poster), *AIChE, Indianapolis*, Nov 2002.

60. Gupta, V. B., Kothari, V. K., Manufactured Fiber Technology, Chapman & Hall, 1997

61. Ziabicki, A., Fundamentals of Fiber Formation: The Science of Fiber Spinning and Drawing, John Willey & Sons, 1976.

62. Heintz, A, Recent Developments in Thermodynamics and Thermodynamics, of Non-Aqueous Mixtures Containing Ionic Lquids, A Review, *Journal of Chemical Thermodynamics*, **37**, 525, 2005.

63. Ritter, S.K., Green Success, *Science and Technology*, **83**(26), 40, 2005.

64. Arlt, W., Seiler, M., Jork, C., New Classes of Compounds for Chemical Engineering: Ionic Liquids and Hyperbranched Polymers, *Technical University of Berlin*, 2003.

65. Namboodiri, V. V., Varma, R. S., Solvent-Free Sonochemical Preparation of Ionic Liquids. *Organic Letters*, **4**(18), 3161, 2002.

66. Bonhote, P., Dias, P. A., Papageorgiou, N., Kalyanasundaram, K., Gratzel, M., Hydrophobic, Highly Conductive Ambient-Temperature Molten Salts, *Inorganic Chemistry*, **35**(5), 1168, 1996.

67. Wilkes, J. S., Properties of Ionic Liquid Solvents for Catalysis, *Journal of Molecular Catalysis A: Chemical*, **214**, 11, 2004.

68. Hermann, W. A., Bohm, V. P., Heck Reaction Catalyzed by Phospha-Palladacycles in Non-Aqueous Ionic Liquids, *Journal of Organometallic Chemistry*, **572**(1), 141, 1999.

69. Howarth, J., Dallas, A., *Molecules*, **5**, 851, 2000.

70. Suarez, P. A. Z., Dullius, J. E. L, Einlofy, S., De Souza, R. F., The Use of New Ionic Liquids in Two-Phase Catalytic Hydrogenation Reaction by Rhodium Complexes, *Polyhedron*, **15**(7), 1217, 1996.

71. Oye, H. A., Jagtoyen, M., Oksefjell, T, Wilkes, J. S., *Material Science Forum*, **183**, 73, 1991.

72. Gordon, C. M., New Developments in Catalysis Using Ionic Liquids, *Applied Catalysis A, General*, **222**(1-2), 101, 2001.

73. Ranke, J, Molter, K. Stock, F., Weber, U. B., Poczobutt, J., Hoffmann, J., Ondruschka, B., Filse, J., Jastorff, B., CPS, Biochem/0303001, at ChemWeb Preprint Server, http://preprint.chemweb.com/biochem/0303001, uploaded13 2003.

74. Swatloski, R. P., Spear, S. K., Holbrey, J. D., Rogers, R. D., Dissolution of Cellulose with Ionic Liquids, *Journal of the American Chemical Society*, **124**, 4974, 2002.

75. Schäfer, T., Rodrigues, C. M., Afonso, C.A.M., Crespo, J. G., Selective Recovery of Solutes from Ionic Liquids by Preevaporation-A Novel

Approach for Purification and Green Processing, *Chemical Communications*, 1622, 2001.

76. Brunner, G., Gas Extraction, Steinkopf, Darmstadt, Springer, New York, 1994.

77. Wang, W., Shen, G., Swatloski, R. P., Farag, R., Broughton, R. M.; Rogers, R. D., Cellulose Fibers Extruded from Ionic Liquids, INTC 2004, Toronto, Canada, September 20, 2004.

78. Doshi, J., Reneker, D. H., Electrospinning Process and Applications of Electrospun Fibers, *Journal of Electrostatics*, **35**(2-3), 151, 1995.

79. Formhals, A., US Patent No. 1975504, 1934.

80. Formhals, A., US Patent No. 2160962, 1939.

81. Subbiah, T., Bhat, G. S., Tock, R. W., Parameswaran, S., Ramkumar, S. S, Electrospinning of Nanofibers, *Journal of Applied polymer Science*, **96**, 557, 2005.

82. Taylor, G. I., *Proc Roy Sco London*, **A313**, 453, 1969.

83. Gibson, P., Schreuder-Gibson, H., Rivin, D., Transport Properties of Porous Membranes Based on Electrospun Nanofibers, *Colloids and Surfaces, A: Physicochemical and Engineering Aspects*, **187-188**, 469, 2001.

84. Dietzel, J. M., Kleinmeyer, J., Harris, D., Beck Tan, N. C., The effect of Processing Variables on the Morphology of the Electrospun Nano Fibers and Textiles, *Polymer*, **42**, 261, 2001.

85. Gibson, P. W., Gibson, H. L., Rivin, D., *AIChe L.*, **45**, 190, 1999.

86. Sundaray, B., Subramanian, V., Natarajan, T. S., Electrospinning of Continuously Aligned Polymer Fibers, *Applied Physics Letter*, **84**(7), 1222, 2004.

87. Koombhongse, S., Liu, W., Reneker, D. H., Flat Polymer Ribbons and Other Shapes by Electrospinning, *Journal of Polymer Science, Part B: Polymer Physics*, **39**(21), 2598, 2001.

88. Kim, J. S., Reneker, D. H., Polybenzimidazole Nanofiber Produced by Electrospinning, *Polymer Engineering and Science*, **39**(5), 849, 1999.

89. Srinivasan, G., Reneker, D. H., Structure and Morphology of Small Diameter Electrospun Aramid Fibers, *Polymer International*, **36**(2), 195, 1995.

90. Kulpinski, P., Cellulose Nanofibers Prepared by the N-Methylmorpholine-N-oxide Method, *Journal of Applied Polymer Science*, **98**, 1855, 2005.

91. Fennessey, S. F., Farris, R. J., Fabrication of Aligned and Molecularly Oriented Electrospun Polyacrylonitrile Nanofibers and the Mechanical Behavior of Their Twisted Yarns, *Polymer*, **45**, 4217, 2004.

92. Theron, S. A., Zussman, E., Yarin, A. L., Experimental Investigation of the Governing Parameters in the Electrospinning of Polymer Solutions, *Polymer*, **45**, 2017, 2004.

93. Baumgarten, P. K., Electrostatic Spinning of Acrylic Microfibers, *Journal of Colloid Interface Science*, **36**(1), 71, 1971.

94. Hayati, I., Bailey, A. I., Tadros, T. F., Investigations into the Mechanisms of Electrohydrodynamic Spraying of Liquids: I. Effect of Electric Field and the Environment on Pendant Drops and Factors Affecting the Formation of Stable Jets and Atomization, *Journal of Colloid Interface Science*, **117**(1), 205, 1987.

95. Buchko, C. J., Chen, L. C., Shen, Y.; Martin, D. C., Processing and Microstructural Characterization of Porous Biocompatible Protein Polymer Thin Films, *Polymer*, **40**(26), 7397, 1999.

96. Megelski, S., Stephens, J. S., Chase, D. B., Rabolt, J. F., Micro and Nanostructured Surface Morphology on Electrospun Polymer Fibers, *Macromolecules*, **35**(22), 8456, 2002.

97. Jaeger, R., Bergshoef, M. M., Martin I. B. C., Schoenherr, H., Vancso, G. J., Electrospinning of Ultrathin Polymer Fibers, *Macromolecular Symposia*, **127**, 216, Feb 1998.

98. Liu, H., Hsieh, Y. L., Ultrafine Fibrous Cellulose Membranes from the Electrospinning of Cellulose Acetate, *Journal of Polymer Science: Part B: Polymer Physics*, **40**, 2119, 2002.

99. Wu, X., Wang, L., Yu, H., Huang, Y., Effect of Solvent on Morphology of Electrospinning Ethyl Cellulose Fibers, *Journal of Applied Polymer Science*, **97**, 1292, 2005.

100.Kim, C. W., Frey, M. W., Marquez, M., Joo, Y. L., Preparation of Submicron-Scale, Electrospun Cellulose Fibers via Direct Dissolution, *Journal of Polymer Science: Part B: Polymer Physics*, **43**, 1673, 2005.

101.Orzada, B. T., Grisset, Collier, B. J., Nonwovens Design Challenge: Fashion Application, *INTC 2005,* 2005.

102.Goff, J., Whelan, T., The Dynisco Extrusion Processors Handbook, 2nd Edition.

103.Wadsworth, L. C., Malkan, S. R., A Review of Melt Blowing Technology, *INB Nonwovens*, 2, 1991.

104.Uyttendaele, M. A. J., Shambaugh, R. L., Melt Blowing: General Equation Development and Experimental Verification, *AIChE Journal*, **36**(2).

105.Bresee, R.R., Ko, W-C, Fiber Formation During Melt Blowing, *INTC 2002 International Nonwovens Technical Conference Proceedings*, Atlanta, 2002.

106.Huang, X., Bresee, R. R., Characterizing Nonwoven Web Structure Using Image Analysis Techniques, Part II: Fiber Orientation Analysis in Thin Webs, *INDA Journal*, **5**(2).

107.Mark, Bikales, Berger, Menges, Encyclopedia of Polymer Science and Engineering, **4**, Second edition, 1990.

108. Annual Book of ASTM Standards (American Society for Testing and Materials), section 7, vol. 7.01, West Conshohochen, PA, 1999.

109. ATS-600 Absorbency Testing System, Thwing-Albert Instrument Company, Brochure dated 03/01.

110. Ayer, Andrew, Sherwood Instruments Inc., Lynnfield, MA, Letter to Larry C. Wadsworth, TANDEC, The University of Tennessee, June 15, 2001.

111.http://www.thwingalbert.com/PDF/2005_PDF/ATS600_Absorbancy_Tester.pdf

112.http://www.pmiapp.com/products/capillary_flow_porometer.html

113. PMI Capillary Flow Porometer, User's Manual, Version 6.0, Ithaca, NY, USA.

114.http://www.kruss.info/techniques/methods_overview_e.html#Dynamische_Wilhelmy

115. Walinder, E. P., Johansson, I., Measurement of Wood Wettability by Wilhelmy Method, Part 1, Contamination of Probe Liquids by Extractives, *Holzforschung*, **55**(1), 21, 2001.

116. Boras, L., Gatenholm, P., Surface Composition and Morphology of CTMP Fibers, *Holzforschung*, **53**(2), 188, 1999.

117. Ghenaim, A., Elchari, A., Louati, M., Caze, C., Surface Energy Analysis of Polyester fibers Modified by Graft Fluorination, *Journal of Applied Polymer Science*, **75**, 10, 2000.

118. Biganska, O., Navard, P., Phase Diagram of Cellulose Solvent: N-Methylmorpholine-N-Oxide Water Mixtures, *Polymer,*

119. Chanzy, H., Nawrot, S., Peaguy, A, Smith, P., Chevalier, J., Phase Behavior of the Quasiternary System N-Methylmorpholine N-Oxide, Water and Cellulose, *Journal of Polymer Science, Polymer Physics Edition*, **20**, 1909, 1982.

120. Kim, D. B., Lee, W. S., Lee, Y. M., Kim, B. C., Effect of Thermal History on the Phase Behavior of N-Methyl Morpholine N-Oxide Hydrates and Their Solutions of Cellulose, *Polymer Journal*, **33**(2), 139, 2001.

VITA

Atul Dahiya was born in Tripoli, Libya, on June 04, 1976. He did his schooling in New Delhi, India. He joined Shivaji University, Kolhapur (India) in August 1996 and received his Bachelor of Textile Plant Engineering in May 2000. In Fall 2001, he joined the Master's program in Textile Science at the University of Tennessee, Knoxville, where he received his degree in August 2003. He continued his study at University of Tennessee, Knoxville in Department of Material Science and Engineering and gained a Ph.D. degree in Polymer and Textile Engineering in May 2006. He was employed as Graduate Research Assistant in the Department of Material Science and Engineering and Textile and Nonwovens Development Center (TANDEC) during his stay at the University of Tennessee.

4502 4346 14
07/20/06 MAB